sustainability

MDPI

Article

Evaluating the Influence of Urban Blocks on Air Pollution Concentration Levels: The Case Study of Golden Lane Estate in London

Mehrdad Borna [1,*], Giulia Turci [2], Marco Marchetti [2] and Rosa Schiano-Phan [1]

[1] School of Architecture and Cities, University of Westminster, London NW1 5LS, UK; r.schianophan@westminster.ac.uk
[2] Architecture Department, University of Bologna, 40126 Bologna, Italy; giulia.turci3@unibo.it (G.T.); marco.marchetti17@studio.unibo.it (M.M.)
* Correspondence: m.borna@westminster.ac.uk

Abstract: Numerous studies have examined the impact of urban form on microclimate and thermal comfort at street level. However, the relationship between air pollution concentration and urban form, particularly vegetation and building arrangement, is less considered among planners and designers, and not many case study examples are available in the literature. To address this gap, this paper provides additional evidence and a case study example, illustrating the impact of the built environment on air pollution in urban areas. The Golden Lane Estate, a residential development that has valuable and repeatable urban design and architectural features and is located near a highly congested and polluted area in central London, was selected as the study site. The analysis involved a combination of fieldwork spot measurements and computational modelling (ENVI-met), considering physical features of urban blocks, levels of air pollution, and meteorological parameters (using data from local meteorological stations). The site modelling simulated current conditions and a condition without vegetation to better understand the impact of vegetation on pollutant concentration. The results indicate that urban form and vegetation arrangements significantly affect wind speed and direction, exacerbating air pollution within street canyons of varying aspect ratios. Such findings contribute to the expanding field of hyperlocal scale measurement and underscore the need for guidelines regarding the optimal placement, scale, type, and distribution of vegetation within street canyons.

Keywords: air pollution; vegetation; urban microclimate; monitoring; modelling; urban form; ENVI-met; particulate matter

Citation: Borna, M.; Turci, G.; Marchetti, M.; Schiano-Phan, R. Evaluating the Influence of Urban Blocks on Air Pollution Concentration Levels: The Case Study of Golden Lane Estate in London. *Sustainability* **2024**, *16*, 696. https://doi.org/10.3390/su16020696

Academic Editor: Mohammad Aslam Khan Khalil

Received: 10 August 2023
Revised: 21 December 2023
Accepted: 9 January 2024
Published: 12 January 2024

1. Introduction

Currently, cities host 57% of the global population. They are expected to play a crucial role in championing innovative and integrated solutions geared towards fostering a climate-responsive and efficient built environment. The EU Recovery Plan [1] emphasises that a pivotal step in this direction involves the retrofitting of the existing building stock, with a specific focus on the neighbourhood scale to interconnect multiple and closely related urban layers (e.g., buildings, infrastructures, greening, mobility, etc.) in ways that positively enhance the quality of the built environment. Additionally, this approach encourages the adoption of participatory methodologies and co-creation mechanisms [2–4], ensuring that the community's concerns regarding the impact of urbanisation and climate change are actively addressed.

City dwellers in low-, middle-, and high-income countries are breathing severely polluted air. In fact, the World Health Organization (WHO), in its announcement in 2018, has stated that nine out of ten people breathe polluted air every day [5]. Additionally, during its first-ever Global Conference on Air Pollution and Health in Geneva in 2018, WHO

announced that these high levels of air pollution constitute the greatest environmental risk to human health. This declaration urged global leaders, governments, policymakers, and stakeholders to take bold actions and implement a range of measures to improve air quality within the next decade [6].

Of particular significance is the district energy production known as Positive Energy Districts (PEDs) and Energy Communities (ECs), which have garnered recognition as emerging neighbourhood models capable of spearheading the transition towards climate-neutral and resilient urban systems [7–9]. These models hold immense potential for improving air quality in urban spaces, as they adopt environmentally conscious practices that minimise pollutant emissions and contribute to cleaner air. By emphasising energy efficiency, renewable energy sources, and sustainable infrastructure, PEDs and ECs play a pivotal role in reducing harmful air pollutants and fostering a healthier urban environment.

In the planning phase of district-scale (neighbourhood) interventions, such as PEDs and ECs, there is an increasing focus on tackling air quality issues as a top priority [10]. According to the Environmental Environment Agency (EEA), air pollution is the most impactful environmental risk on health. Continuative exposure to high levels of fine particulate matter ($PM_{2.5}$) is proven to have a severe impact on human health, causing breathing problems, cardiovascular and pulmonary diseases, lung cancer, and also the highest probability of premature mortality [11]. In particular, the elderly, children, and people with pre-existing health problems are more vulnerable to the health impacts of air pollution [12]. Efforts are directed towards implementing measures that mitigate emissions, enhance air circulation, and create green spaces that act as natural filters, thereby purifying the air in the urban environment. It is, therefore, important to understand the impact of urban form and activities on air velocity and circulation [13], and how parameters such as greenery, trees, and vegetation can be effectively used to reduce air pollution within urban spaces [14,15]. This proactive approach in the early stages of development ensures that air quality considerations are seamlessly integrated into the neighbourhood's fabric, leading to sustainable and breathable urban spaces.

In Europe, despite the implementation of several efforts by central governments—i.e., EU quality standards to protect human health and the environment (https://environment.ec.europa.eu/topics/air/air-quality_en (accessed on 15 July 2023))—city planners, and local agencies, urban dwellers are still exposed to unacceptable levels of pollutant concentrations. These levels exceed the national and international legal air quality obligations and objectives set by the EEA and the WHO. Dense urban areas, in particular, face higher air pollution concentrations compared to the outskirts and surrounding areas [16]. The major sources of air pollution in cities are traffic emissions and domestic fuel burning. In these cases, the dense urban setting hinders wind flow, resulting in air stagnation. This stagnation allows pollutants emitted from vehicle exhaust and chimney smoke to accumulate, exacerbating air pollution within the inner parts of cities. Air pollution poses a clear problem for human health and the environment. In response, numerous mitigation strategies have been proposed or already implemented. As such, in recent years, the use of trees to improve air quality has gained increasing recognition as an effective strategy for removing or dispersing pollutants [17–22].

Many municipalities consider urban trees, vegetation barriers, green walls, and green roofs as effective urban planning solutions to improve liveability and enhance air quality in urban areas [23]. The positive impact of urban green infrastructures has been extensively studied, particularly in relation to the Urban Heat Island Effect (UHIE). These green elements provide shade and evapotranspiration, which can reduce surface temperatures and peak summer air temperatures by 1–5 °C [24–26]. According to Livesly et al. [27], well-arranged networks of green open areas cutting through the entire built-up area can regulate the local wind caused by the city's Heat Island Effect. This not only creates more pleasant spaces between buildings for urban dwellers but also enhances the quality of outdoor areas by improving pedestrian thermal comfort and encouraging people to spend time outside and engage with their environment on various levels. In addition to these benefits, urban

green infrastructure offers other advantages, such as reducing water runoff through canopy interception during rainfall [28–30]; lowering building energy loads by strategically planting trees to provide shade and reduce air-conditioning usage, thereby lowering greenhouse gas emissions [31–33]; attenuating noise through vertical greenery systems [34–36]; and enhancing the quality of outdoor spaces through the botanical, aesthetic, and social value of green spaces [37–48].

Regarding air pollution, numerous studies suggest that trees mitigate air pollution through the deposition of particulate matter [49–51]. However, it should be noted that increasing the number of trees and vegetation can modify the urban form, which directly impacts the urban microclimate. This modification can have a pronounced effect on urban wind flow and air volume, leading to a decrease in air velocity around trees. As a result, the dilution rate and air exchange are reduced, potentially leading to higher concentrations of pollutants at the hyperlocal scale at the pedestrian level [52]. The positive impact of trees on improving air quality is primarily linked to two main features. First, trees absorb gaseous pollutants, such as CO_2, NOx, O_3, and SO_2, through the stomata on their leaves. Second, vegetation has the capacity to trap fine particulates on its leaves and bark. The effectiveness of these benefits depends on various factors, including the type of pollutant particles (size and shape), characteristics of the green infrastructure (species, arrangement, porosity, foliage), and meteorological parameters (wind flow velocity and direction, air temperature, and relative humidity). To date, many studies have used deposition models [47,53–55] to estimate the capacity of vegetation to remove pollutants. However, the effects of urban forests in terms of reducing pollutant concentrations are found to be rather limited, with reductions of up to about 2%. Having said that, there may be slightly higher deposition in the summer due to a larger leaf area density [56].

The mitigative effect of urban greenery on air pollution is only one aspect of the equation; however, urban vegetation can also have a negative effect by increasing local air pollutant concentrations [15,57]. It has been demonstrated that, under certain circumstances, trees acting as obstacles in an urban setting can reduce wind velocity and result in an increase in pollutant concentrations at the pedestrian level. Several studies [58–60], utilising wind tunnel experiments and Computational Fluid Dynamics (CFD) simulations, have confirmed that this issue is particularly prominent along urban street canyons. It mainly depends on factors such as wind direction and speed, the aspect ratio of the street canyons (W/H = Width/Height), and to a lesser extent, the arrangement of tree plantings and foliage density. However, it is necessary to reconsider the general notion that planting trees on streets with moderate traffic can always be considered as an effective strategy for reducing air pollution levels.

As mentioned earlier, there are numerous variables that influence and determine urban air quality. Therefore, in addition to considering green infrastructure, we should also take into account the form and geometry of buildings, as they can significantly impact the retention or dispersion of pollutants [61–63]. Based on these findings, in order to enhance the dispersion of air pollution in outdoor spaces, we need to assess both the effects of vegetation layout and building arrangements using specific methods tailored to each particular case.

Within this perspective, the present study investigates the concentration and dispersion patterns of outdoor air pollution in a real residential urban block in London. The aim is to document how air pollution concentrations are influenced by the built form and vegetation within the area. It should be noted that this paper focuses on a single meteorological and climatic condition, and a comprehensive assessment would require an extended analysis encompassing different environmental and weather conditions over the course of a year. In the following sections, this paper describes the main objectives, the methodology adopted, the key findings, and the potential for future studies.

2. Aims and Objectives

This research investigates the concentration of air pollution within an existing residential city area using fieldwork analysis and computational modelling. The Golden Lane Estate, located in central London, was chosen as a case study due to its proximity to one of the most congested and polluted areas in the city. The housing development has unique characteristics that create sheltered residential blocks with a population density of 500 p/ha [64] and an inward configuration, resulting in a series of courtyards, protected green spaces (including grass and trees), and microclimates [65,66]. In the context of Golden Lane's "city within the city" layout, several questions arise regarding the potential role of the urban form in influencing, not only outdoor thermal comfort, but also the air quality within the enclosed urban spaces. Therefore, the following specific objectives were defined for this study:

1. To measure and monitor the impact of green infrastructure (GI) and building arrangements on the concentration and dispersion of air pollutants (specifically, $PM_{2.5}$, PM_{10}, and NO_2).
2. To assess and better understand the relationship between the dispersion of air pollutants ($PM_{2.5}$, PM_{10}, and NO_2) and meteorological parameters, such as air temperature, relative humidity, and wind velocity, thereby providing detailed insights into the complex nature of the air quality dynamics in the study area.

3. Methodology

To ensure broader applicability of the results, this study selected a typical building configuration that represents the conditions and characteristics commonly found in various built settlements across cities with high, medium, and low densities. Based on the Local Climate Zone (LCZ) scheme developed by Stewart and Oke [67], the site can be classified as an "Open high-rise (LCZ 4)" area with an aspect ratio ranging from 0.75 to 1.25. The open high-rise is one of the 10 LCZs defined by Stewart and Oke. It is characterised by tall buildings (taller than 25 m) that are widely spaced, with large areas of exposed ground or water between them. Similarly, the selected site consists of tall buildings, spanning several stories, with an open arrangement and access to a reasonable amount of green infrastructure and scattered trees. The chosen case study site underwent a comprehensive analysis, combining fieldwork measurements with computational modelling and simulation. This analysis considered both the levels of air pollutants and meteorological parameters, such as air temperature, relative humidity, and wind velocity. Additionally, urban physical features, such as buildings' geometry, voids/open spaces, and green spaces, were recorded and documented. In the modelling process, besides the current conditions (with vegetation), a scenario without vegetation was also simulated to better understand the relationship between vegetation and pollutant concentrations.

3.1. Case Study Selection and Description: Golden Lane Estate

Golden Lane Estate was constructed in the northeast part of the City of London after the Second World War on a site that had been heavily damaged by bombings. The Estate's design was the outcome of an architectural competition with the aim of creating high-density, affordable modern housing for individuals working in the city (see Figure 1, left). The competition's winning design was submitted by Jeffry Powell. Following this, three young architects—Chamberlin, Powell, and Bon—decided to collaborate and form Chamberlin, Powell, and Bon (CP&B) to develop the final built scheme [64]. Modernist architecture greatly influenced this project, as the architects adopted an innovative design approach that diverged from traditional urban forms, such as rows of houses along streets. Instead, they created self-contained blocks organised around predominantly communal spaces.

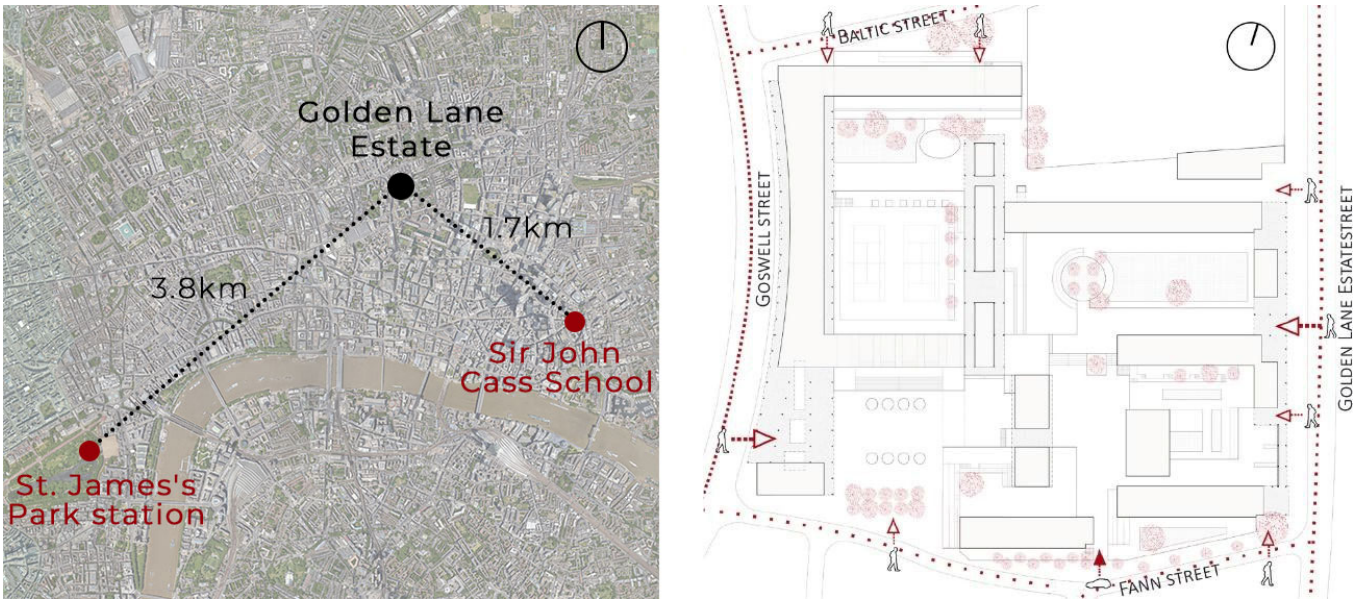

Figure 1. (**left**) Case study: Golden Lane Estate satellite view, (**right**) Golden Lane Estate plan overview.

The residential blocks within Golden Lane Estate are arranged perpendicular to each other, creating a dynamic succession of outdoor space organised in a series of characteristic courtyards. These blocks are supported by a public ground that contributes to the formation of sunken and canted spaces (see Figure 1, right). At the podium level, there are several passages, both physical (serving as various access routes to the Estate) and visual (providing opportunities to see inside), which enhance the permeability of this area and promote its continuous use. To revitalise the area and foster a greater sense of belonging and hope among the residents, the facades of the Estate feature cladding panels in different colours. Taking inspiration from Le Corbusier, primary colours were used: red and blue panels adorn the main facades of the maisonettes, while Great Arthur House, the tallest building, incorporates a curtain wall finished with yellow Pilkington glass.

The Golden Lane Estate is surrounded by four streets. The busiest street among the four is Goswell Road, running in a north–south direction, with an average daily flow of 14,904 vehicles per year [68]. Golden Lane Street and Baltic Street experience a moderate level of traffic, while Fann Street, being a one-way road, has relatively low traffic. The main pedestrian accesses are located on Goswell Road and Golden Lane, while the only vehicle access to the inner courtyard is via Fann Street. Information related to vegetation characteristics, such as species name, height, crown shape/size, clear stem height, Leaf Area Density (LAD), leaf persistence, and surface cover, is described in Table 1. The greenery properties and associated details were obtained from a number of previous studies [22,58,69–74] and cross-checked by fieldwork observation.

3.2. Fieldwork: On-Site Spot Measurements

In order to gain a comprehensive understanding of the outdoor microclimatic conditions at the site, selected points were identified, and measurements were conducted. A multi-function vane meter equipped with a thermometer, hygrometer, and anemometer (refer to Table 2) was utilised to assess air temperature, relative humidity, and wind velocity. The instrument is compact and lightweight, and capable of measuring temperatures from 0 °C to 50 °C (with a resolution of 0.1 °C), relative humidity from 10% to 95% RH (with a resolution of 0.1% RH), and wind speeds from 0.4 m/s to 30.0 m/s (with a resolution of 0.1 m/s).

Table 1. Vegetation characteristics and location in Golden Lane Estate.

Location and Vegetation Image Number	Vegetation Scientific Name	Vegetation Common Name	Vegetation Height (Top of Vegetation from Ground) (m)	LAD (High/Low)	Typology (Ever-green/Deciduous)	Trunk Size (Small/Medium/Large)	Crown Shape (Cylindrical/Heart-Shape/Spherical	Clear Stem Height (m)
A	Carpinus	Hornbeam	5–7	High	Deciduous	Medium	Broadly Oval (Heart-Shaped)	2–3
B	Catalpa bignonioides	Indian-bean-tree	9	Low	Deciduous	Medium	Broadly Round (Spherical)	4–5
C	Pyrus	Pear	4–5	High	Deciduous	Medium	Irregular (Heart-Shaped)	1–2
D	Prunus avium	Cherry Tree	8–10	Low	Deciduous	Medium	Irregular (Heart-Shaped)	2.5
E	Acer saccharinum	Silver Maple	10	High	Deciduous	Large	Broadly Oval (Heart-Shaped)	2
F	Betula pendula	Silver birch	11	Low	Deciduous	Medium	Irregular (Heart-Shaped)	1
G	Fagus	Beech Tree	12	High	Evergreen	Large	Broadly Oval (Heart-Shaped)	0.5
H	Crataegus persimilis	Broad-leaved cockspur thorn	3	Low	Deciduous	Small	Irregular (Heart-Shaped)	1.5
I	Cherry Laurel	Prunus laurocerasus	3–4	High	Evergreen	N/A	Hedge	0
L	Ficus carica	Fig	5	High	Deciduous	Medium	Broadly Round (Spherical)	1.5
M	Cedrus deodara	Deodar	12	Low	Evergreen	Medium	Irregular (Pyramidal)	2
N	Malus domestica	Apple	6	High	Deciduous	Small	Broadly Oval (Heart-Shaped)	1
O	Laurus	Bay	2	High	Evergreen	N/A	Hedge	0
P	Pittosporum tenuifolium	Kohuhu	2.5	High	Evergreen	N/A	Hedge	0
Q	Cercis siliquastrum	Judas-tree	5	Low	Deciduous	Medium	Broadly Round (Spherical)	2
R	Platanus	Plane	22	Low	Deciduous	Large	Broadly Oval (Heart-Shaped)	3

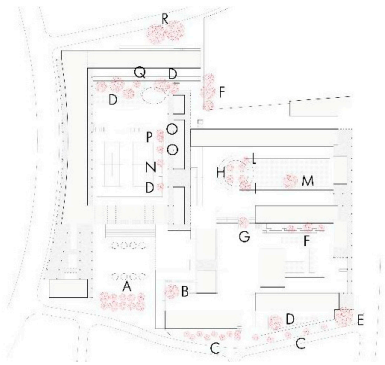

A—Hornbeam
B—Indian-bean-tree
C—Pear
D—Cherry Tree
E—Silver Maple
F—Silver birch
G—Beech Tree
H—Broad-leaved cockspur thorn
I—Prunus laurocerasus
L—Fig
M—Deodar
N—Apple
O—Bay
P—Kohuhu
Q—Judas-tree
R—Plane

Table 2. Aeroqual Series 300—Type and manufacturer.

System Specifications	
Measurement units	Gas: ppm or mg/m^3 | Humidity: % | Temperature: °C or °F
Reading functions	Instant, minimum, maximum, average
Sensor head	Active fan sampling accuracy measurements, interchangeable
Sensor head calibration	Zero and span calibration
Temperature and humidity sensor	Range −40 °C to 124 °C (−40 °F to 255 °F); Range 0 to 100% RH
Environmental operating conditions	Temperature: −5 °C to 45 °C | Humidity: 0 to 95% non-condensing
Display status indicators	Battery, sensor, standby
Enclosure material and rating	PC and ABS; IP20 and NEMA 1 equivalent
Size	(L × W × D) 195 × 122 × 54 (mm)
Weight	<460 g (with sensor head and battery)
Approvals	Part 15 of FCC Rules

To measure the concentration of air pollutants, such as $PM_{2.5}$, PM_{10}, and NO_2, in real time at specific locations, an Aeroqual portable air quality monitor device (refer to Table 3) was employed. The device utilises interchangeable "sensor heads" attached to the monitor base to facilitate spot measurements. There are 27 different sensor heads available, each containing a single gas or particle sensor. Swapping sensor heads does not necessitate configuration or re-calibration. Nevertheless, all sensor heads were calibrated by co-locating them alongside a reference monitoring station of higher accuracy prior to the measuring day.

Table 3. Australian Scientific LM-8000A—Type and manufacturer.

System Specifications	
Measurement	Anemometer, Humidity, Temperature, Light
Air velocity	Range: 0.4 to 30.0 m/s | Resolution: 0.1 m/s
Humidity	Range: 10 to 95% RH | Resolution: 0.1% RH
Temperature	Range: 0 to 50 °C | Resolution: 0.1 °C
Light	Range: 0 to 20,000 Lux | Resolution: 1 Lux
Weight	160 g (battery included)
Dimension	HWD 156 × 60 × 33 mm

All measurements were gathered on a partially sunny autumn day (25 October 2018) between the hours of 13:00 and 16:00, with a reference height of 1.5 m above ground level. The study subsequently adapted and applied the following method to collect and analyse the acquired data:

- Single values were recorded for air temperature (°C) and relative humidity (%);
- Minimum and maximum values were recorded in a 3 min interval for wind speed (m/s);
- Average values were recorded for $PM_{2.5}$, PM_{10}, and NO_2 ($\mu g/m^3$);
- Selected points are shown in Figure 2, and detailed measurement results are reported in Table 4.

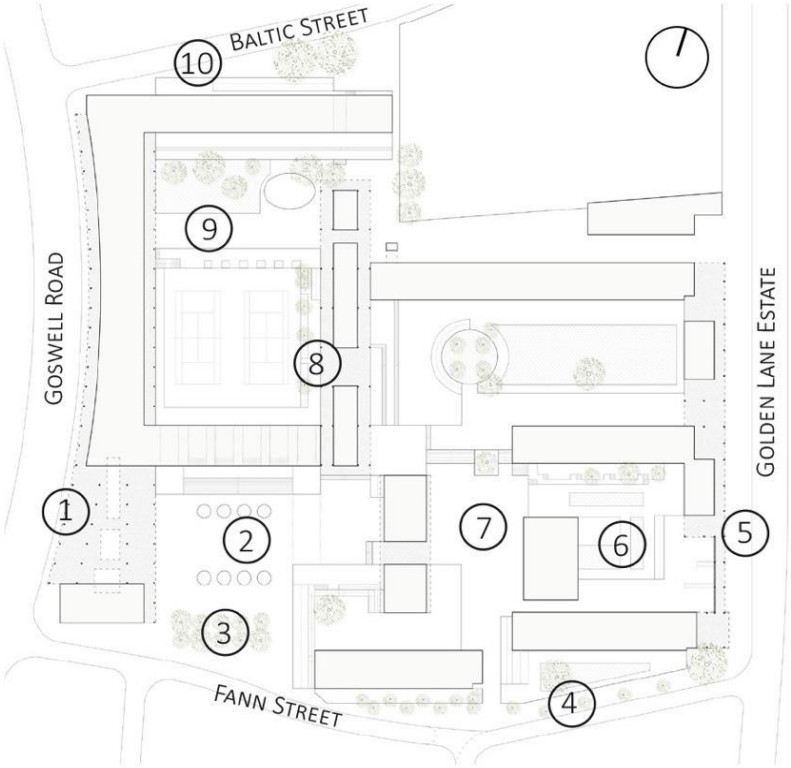

Figure 2. Ten selected measurement spots on the map, each marked with a circled number.

Table 4. Measurements were taken in Golden Lane Estate on 25 October 2018.

SPOT	TIME (h)	T (°C)	RH (%)	WS MIN–MAX (m/s)	WS AVER. (m/s)	$PM_{2.5}$ ($\mu g/m^3$)	PM_{10} ($\mu g/m^3$)	NO_2 ($\mu g/m^3$)
Spot 1	13:54	17.6	52.3	0.0–0.5	0.3	8	10	18
Spot 2	14:02	15.9	57.2	0.8–1.3	1.1	8	9	12
Spot 3	14:06	15.0	59.2	0.7–1.8	1.3	8	9	19
Spot 4	14:21	14.2	62.3	1.8–2.1	2.0	8	9	23
Spot 5	14:24	14.9	60.0	0.0–0.5	0.3	7	8	13
Spot 6	14:32	14.7	60.7	0.7–1.0	0.9	6	7	15
Spot 7	14:36	14.0	63.2	1.5–2.0	1.8	7	8	13
Spot 8	14:50	14.8	60.7	0.4–0.8	0.6	9	10	16
Spot 9	14:58	14.5	62.1	0.4–0.8	0.6	8	10	14
Spot 10	15:17	14.7	61.6	0.9–1.3	1.1	7	8	12

Data related to street-level road traffic and road length, as well as information about buildings' form, including height and geometry, vegetation type and size, and surface materials, were recorded and collected using a combination of conventional field measurements, satellite-based measurements, road traffic counts from the Department for Transport, and official GIS documents/maps provided by Ordnance Survey, the UK's governmental mapping agency. The data collected from official GIS sources were cross-checked and verified against conventional field measurements. In certain instances, aerial perspectives from Bing Maps and Google Maps were utilised to reduce the potential for errors.

3.3. Computer Modelling and Simulation Configuration

Evaluating urban microclimate conditions requires considering numerous interrelated parameters, including buildings' form and their typology, materials, and vegetation, as well as their distribution, local microclimate conditions (temperature, relative humidity, wind direction and speed), and pollutant dispersion and concentration. To account for all these variables, simulations were conducted using the comprehensive modelling and simulation application ENVI-met v.4.4.

ENVI-met is a three-dimensional non-hydrostatic microclimate model that employs the fundamental principles of fluid dynamics and thermodynamics to calculate and simulate microclimates in urban areas. The model solves the differential equations on a staggered grid system using the finite difference method and incorporates Reynolds-averaged Navier–Stokes (RANS) equations to parameterise turbulent flows. Typical grid resolutions range from 0.5 to 10 min space, with a time step of 1 to 5 s. This level of resolution enables the analysis of interactions among individual buildings, surfaces, and plants at different scales [75].

The application structure of ENVI-met can be divided into three parts: input, simulation, and output. Once input data, such as site configuration, location, climatic conditions, and the investigation period, are entered, ENVI-met applies calculation models and equations to run the simulation. The results are organised into folders containing various output files, which can be read and analysed using a tool within ENVI-met called Leonardo. Leonardo enables the visualisation of the spatial distribution of specific microclimate variables and pollutant dispersion using Outdoor Microclimate Maps (OMMs). In the specific context of this research, the ENVI-met input data are summarised in the following tables (refer to Tables 5 and 6).

Table 5. Golden Lane Estate input file.

SIMULATION AREA FILE (.inx)		**CONFIGURATION FILE (.sim)**	
Localisation, lat. (deg,+N,−S):	51.52	- Start and duration of model	
	−0.09	run	25.10.2018
long. (deg,−W,+E):	130 × 130 × 60	. start date (DD.MM.YYYY):	07:00:00
- Grid dimension (x, y, z):	2 m; 2 m; 1.5 m	. start time (hh:mm:ss):	12
- Grid cells size (dx; dy; dz):	5	. total simulation time (h):	
- Nesting grids (Nr):		- Initial meteorological	2.5
- Space configuration	Google Maps and survey on	conditions	260
. DEM configuration:	site	. wind speed at 10 m height	10.11
	Google Maps and survey on	(m/s):	69
. buildings configuration:	site	. wind direction (deg):	data by www.rp5.ru (accessed
	Google Maps and survey on	. initial temperature (°C)	on 25 October 2018)
. soil typology:	site	. relative humidity in 2 m (%):	multi-pollutant
	Google Maps and survey on	- Hourly meteorological	(NO, NO_2, O_3, PM_{10} and
. vegetation typology	site	conditions:	$PM_{2.5}$)
and configuration:	Google Maps and survey on		active chemistry
. sources of pollutants:	site		
	www.londonair.org.uk	- Pollutants dispersion and	
. geometry:	(accessed on 1 November	reactions	
	2018),	. operation mode:	
. height (m):	Google Maps and survey on		
	site	. chemistry.	
	0.5		

Table 6. London meteorological conditions and pollutants concentrations. The considered stations are the nearest to the study area available on the reference websites.

Meteorological Conditions on 25 October 2018, Weather Station London St. James' Park and www.metoffice.gov.uk (accessed on 1 November 2018)					**Pollutants Concentration on 25 October 2018, Station London Sir John Cass School (NO; NO_2; PM_{10}; $PM_{2.5}$) and Bloomsbury (Ozone)**				
Hourly Time (UTC)	**Air Temperature (°C)**	**Rel. Humidity (%)**	**Wind Velocity (m/s)**	**Wind Direction**	**NO (μg/m³)**	**NO_2 (μg/m³)**	**Ozone (μg/m³)**	**PM_{10} (μg/m³)**	**$PM_{2.5}$ (μg/m³)**
00:00:00	9.50	82	2	SW	3.70	25.40	31.90	23.00	9
01:00:00	7.50	90	2	W	3.20	27.80	28.10	19.40	6
02:00:00	7.00	95	2	WNW	3.80	34.40	25.90	24.40	3
03:00:00	6.70	96	2	W	4.00	34.00	22.00	22.00	5
04:00:00	6.60	95	1	WSW	9.80	46.50	16.40	22.20	9
05:00:00	6.10	97	1	WSW	24.90	50.4	3.80	22.40	11
06:00:00	5.90	97	1	W	49.30	54.80	1.20	26.80	13
07:00:00	6.60	97	2	W	42.60	57.70	1.60	28.20	13
08:00:00	7.30	95	2	W	35.50	57.10	6.00	38.20	10
09:00:00	9.00	87	3	NW	37.20	55.30	13.20	28.80	16
10:00:00	10.80	78	4	NNW	30.90	49.70	22.60	29.40	13
11:00:00	12.60	69	4	NW	19.50	42.20	30.30	23.40	9
12:00:00	14.10	66	3	NNW	12.10	34.20	26.70	22.40	17
13:00:00	14.60	65	4	W	14.30	42.40	36.50	18.80	9
14:00:00	13.50	67	3	W	17.10	47.10	28.90	19.00	8
15:00:00	13.30	70	3	NW	27.70	59.30	20.00	21.60	11
16:00:00	13.20	70	4	WNW	19.30	61.20	11.20	18.20	12
17:00:00	12.20	72	4	NW	8.70	43.10	17.60	17.20	8
18:00:00	11.90	71	3	NW	11.40	41.10	26.30	17.20	9
19:00:00	11.60	73	4	NW	7.50	35.80	24.30	16.80	9
20:00:00	10.90	77	3	NW	12.80	33.30	30.70	14.60	8
21:00:00	10.60	78	3	WNW	6.30	27.70	26.50	8.60	7
22:00:00	10.50	78	3	WNW	6.30	27.30	37.70	9.40	6
23:00:00	10.60	73	3	W	7.60	28.70	35.50	8.20	7

To increase accuracy and minimise the influence of initialisation and convergence errors, the simulation was run for 6 h before and after the sampling period, as recommended by Salata et al. [76]. Therefore, a 12 h simulation cycle was chosen. Since the field spot measurements were conducted for only one and a half hours, data from the closest air monitoring station to the site were used to fill in the missing data for the total simulation

time of 12 h. The selected time for comparing computational modelling and field spot measurements was 15:00 (UTC). This temporal selection aligns with the midpoint of the spot measurement window, ensuring meaningful synchronisation between the model output and on-site measurements. The values obtained from our spot measurements provided insights into the behaviour and concentration of air quality at different locations within the site. Similarly, our simulation model concentrated solely on pollution concentration at a specific time rather than the pollution levels. As outlined in the aims and objectives, this paper primarily investigates the influence of the urban microclimate on air pollution concentration, diverging from a focus on pollution levels. Despite potential limitations in capturing temporal variations with only one record for variables sampled at different locations, a singular representative hour not only facilitates a concise examination of the model's performance but also provides valuable insights into comparative aspects of pollutant concentration. This approach sheds light on spatial patterns, contributing meaningfully to the research objectives.

Two air monitoring sites were identified near the site: 'City of London—Beech Street', located approximately 300 m way, and 'City of London—Sir John Cass School' about 1.7 km (1700 m) away. After careful examination and comparison, the data from the 'City of London—Sir John Cass School' air quality station were selected for use in this study. This station provided data on the key urban pollutants of interest, namely, NO_2, PM_{10}, and $PM_{2.5}$.

Furthermore, the 'Sir John Cass School' (Figure 1) monitoring site is categorised as 'Urban Background' and differs from Kerbside and Roadside monitoring sites in that it is not dominated by a single nearby pollution source. Urban background monitoring sites are designed to capture the ambient pollution level, which can be attributed to multiple sources, such as vehicle traffic, airports, car parks, gas boiler flues, and nearby construction sites. Typically, these sites are located approximately 50 m away from major pollution sources and more than 30 m way from busy roads. Extracting data from such a monitoring site provides a better representation of a typical residential area, with similarities in microclimate and pollution exposure to our study site. For meteorological parameters, such as air temperature (°C), relative humidity (%), and wind velocity (m/s), data from the closest station to the site, St. James' Park station, located 3.8 km (3800 m) away (Figure 1), were used.

It is important to note that ENVI-met models are not reliable at their model borders and in close proximity to them. To ensure accuracy and numerical stability of the simulation results, the nesting area of all simulation scenarios was chosen to be sufficiently large. A nesting area refers to a more localised and higher-resolution subdomain intricately incorporated within a broader and coarser-resolution subdomain. This method is employed to enhance simulation accuracy in specific areas of interest, such as around buildings or within vegetated areas. Following the guideline prescribed by Conry et al. [77], five nesting grid cells (Figure 3) were set on each side of the model. Additionally, based on Erel et al. [78], the z-grid was set to three times the height of the tallest building in the model site.

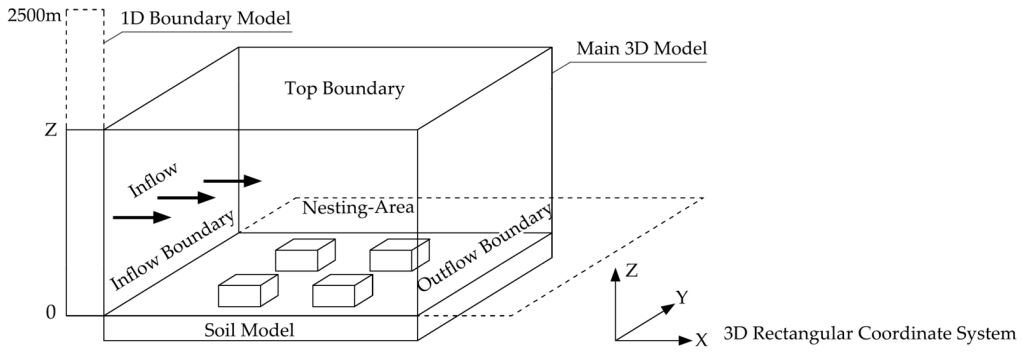

Figure 3. Basic architecture of ENVI-met v.4.4 software model layout and the extent of nesting area.

The results of the ENVI-met simulation were subsequently compared with the field spot measurement values. Further analysis and validation are provided in the Results and Discussion sections of this paper.

The scenarios that were modelled and simulated represent the current conditions of the site, including the existing and unchanged configuration of buildings and vegetation. However, to gain a better understanding of the relationship between vegetation and pollutants dispersion, a no-vegetation scenario was also simulated for both areas. The input files for this scenario remained unchanged, except for the removal of vegetation from the model.

4. Results

Microclimate variables and pollutant dispersion were investigated at 15:00 on 25 October 2018 and represented in vertical and horizontal sections at a height of 1.5 m above the terrain. The applied methodology yielded different outcomes: on-site measurements provided spot values at specific points, while ENVI-met simulations, using Outdoor Microclimate Maps (OMMs), allowed for visualising the spatial distribution of values across the Estate. To facilitate direct comparison of the results, an analogous colour scale was employed for each analysed variable in both methods: light colours corresponded to lower values, while dark colours indicated higher values.

The results are presented for the analysed microclimatic variables and pollutant dispersion values, including temperature, relative humidity, wind velocity, $PM_{2.5}$, PM_{10}, and NO_2. For each variable, three images are provided. The left image displays the visualisation of spot measurements, and the central image shows the scenario based on the OMM obtained from the ENVI-met simulation, representing the existing situation. The right image illustrates the no-vegetation scenario, also based on the OMM obtained from the ENVI-met simulation.

4.1. Air Temperature (°C)

The three images allow us to assess the distribution of air temperature (°C) in the outdoor spaces of Golden Lane Estate (Figure 4). By comparing the images, we can observe that the air temperature is relatively uniform throughout the site, with a temperature difference of approximately 2 °C between the warmer and cooler areas, as indicated by both spot measurements and OMMs. Courtyard 1 and Courtyard 4 exhibit higher air temperature values, while a slight temperature reduction can be observed under the covered pedestrian passages connecting Goswell Road to Courtyard 1 and Courtyard 1 to Courtyard 4. The lowest temperature was recorded beside the block adjacent to Fann Street.

Since this assessment took place at 15:00 in October, a portion of solar radiation was blocked by the tall buildings situated on the southern part of the site (opposite Fann Street), casting long shadows. The temperature in this area further decreased due to the presence of rows of low-height trees.

Focusing on the analysis of the current scenario depicted in the left and central images (Figure 4), a consistent pattern of air temperature distribution can generally be observed. However, the value measured under the covered walkway connecting Goswell Road to Courtyard 1 appears to be inconsistent with the ENVI-met simulation result. This discrepancy is believed to be due to direct solar radiation exposure during the fieldwork.

When comparing the current scenario with the no-vegetation scenario simulated using ENVI-met, the presence of greenery does not significantly influence air temperature values. The only notable variation is observed along Fann Street, where the presence of trees leads to a decrease in temperature values (due to evaporative cooling and the shading effect of tree crowns).

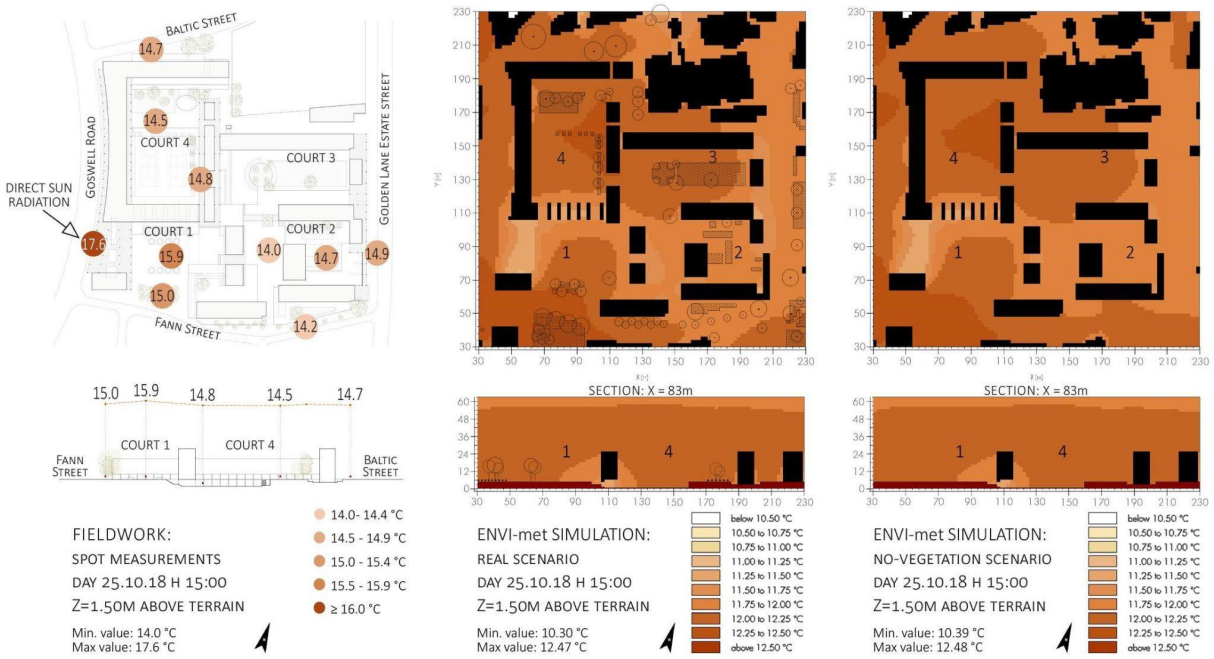

Figure 4. Air Temperature (°C): (**left**) Fieldwork measurement, (**centre**) ENVI-met current scenario simulation, (**right**) ENVI-met no-vegetation scenario simulation.

4.2. Relative Humidity (%)

The images depict the distribution of relative humidity (%) in the outdoor spaces of Golden Lane Estate (Figure 5). Upon comparing the fieldwork measurements and OMMs, no significant variations in relative humidity values are observed. The maximum difference, evaluated through both spot measurements and OMMs, is less than 5%.

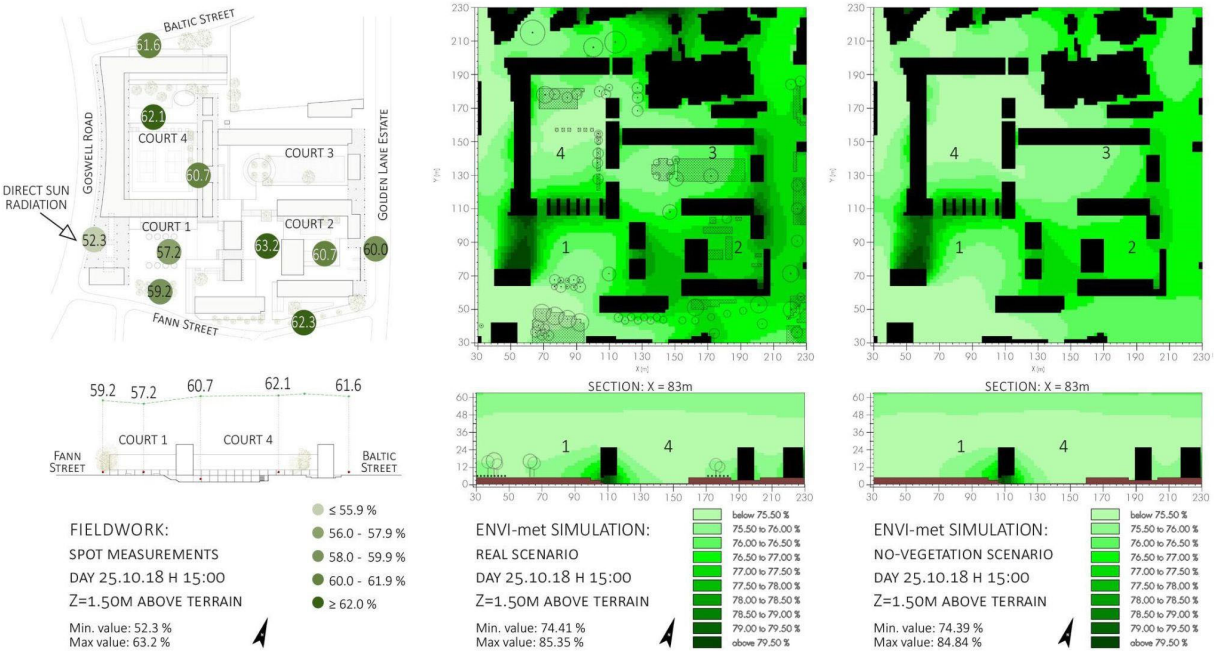

Figure 5. Relative Humidity (%): (**left**) Fieldwork measurement, (**centre**) ENVI-met current scenario simulation, (**right**) ENVI-met no-vegetation scenario simulation.

The analysis reveals a close correlation between air temperature and relative humidity distribution. By observing the ENVI-met simulations at 15:00 (Figures 6 and 7), it becomes

apparent that areas with higher relative humidity values correspond to areas with lower air temperature values, and vice versa. ENVI-met Outdoor Microclimate Maps, representing the real scenario and the no-vegetation scenario, emphasise how the presence of green canopies along Fann Street and Golden Lane Street contributes to increased relative humidity values in the surrounding areas. To a lesser extent, the presence of a water pool in Courtyard 2 and the existence of grass in Courtyard 3 and Courtyard 4 also contribute to a higher percentage of relative humidity when compared to a scenario without vegetation.

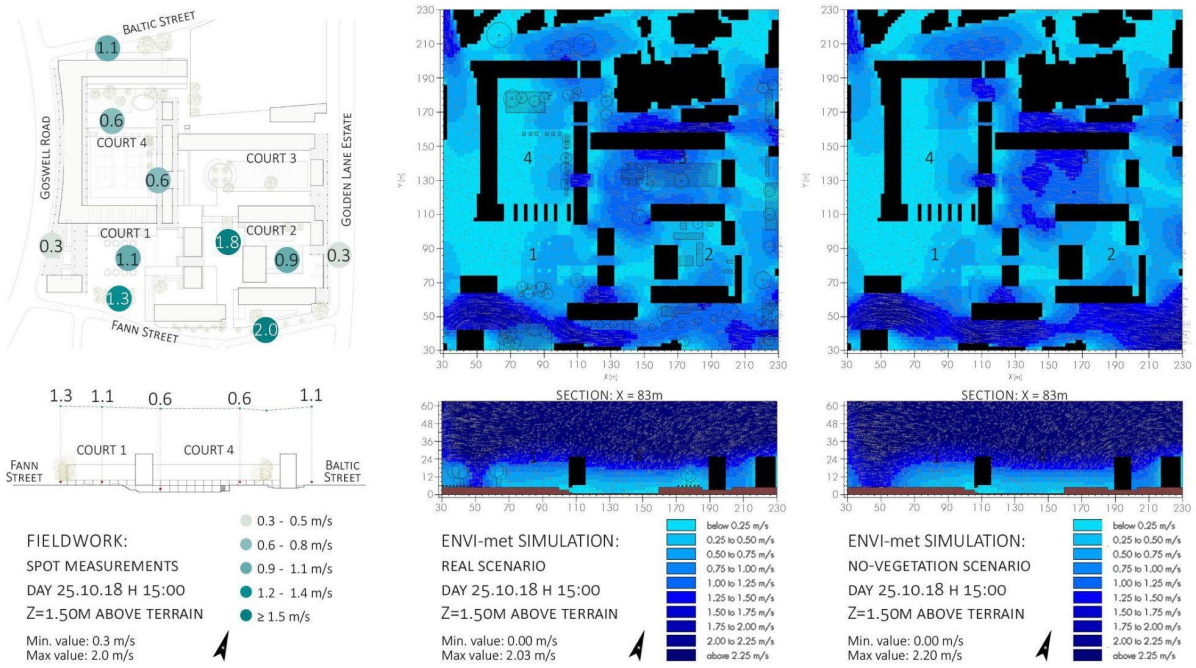

Figure 6. Wind Velocity (m/s): (**left**) Fieldwork measurement, (**centre**) ENVI-met current scenario simulation, (**right**) ENVI-met no-vegetation scenario simulation.

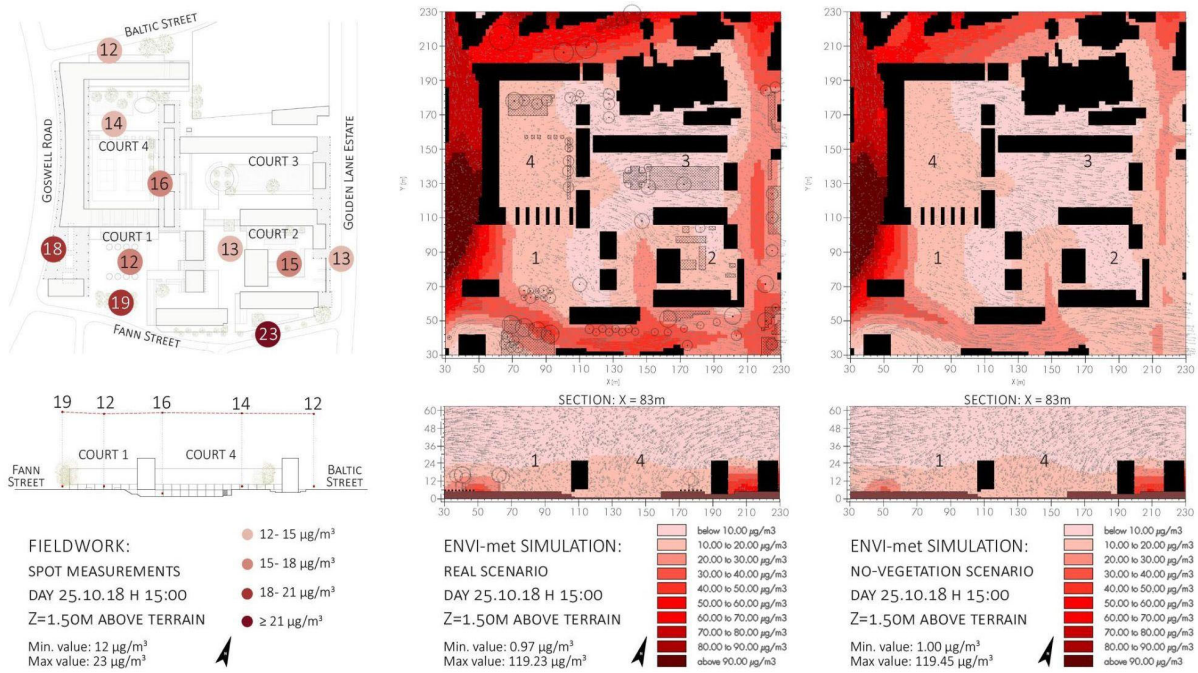

Figure 7. NO_2 concentration (µg/m^3): (**left**) Fieldwork measurement, (**centre**) ENVI-met current scenario simulation, (**right**) ENVI-met no-vegetation scenario simulation.

4.3. Wind Velocity (m/s)

The three images provide visualisations of wind velocity (m/s) and, in the case of ENVI-met simulations, wind direction in the outdoor area of Golden Lane Estate (Figure 6). Based on fieldwork measurements and meteorological data used for ENVI-met simulations, the prevailing wind flow on the specified date was from the southwest to the northeast direction. The images demonstrate that wind velocity is closely influenced by the layout of the site and the configuration of streets. Narrow passages and street sections with a low height-to-width ratio result in an increase in airflow speed. In the case of Golden Lane Estate, this phenomenon is observed along Fann Street and in the covered passages connecting Courtyard 1 to Courtyard 2 and Courtyard 3 to Courtyard 4, where the airflow is constrained, leading to the highest values of air velocity.

By comparing fieldwork measurements and the real scenario simulation in ENVI-met, depicted in the right and central images, a positive correlation in the pattern and values of wind velocity is evident. The arrangement and disposition of trees have a significant impact on airflow direction and velocity. The analysis of the current and no-vegetation scenarios simulated by ENVI-met demonstrates how the presence of trees acts as an obstacle to airflow, resulting in a noticeable decrease in wind velocity. This effect is particularly prominent in Fann Street, where a dense tree canopy obstructs the regular airflow and reduces wind velocity compared to a scenario without vegetation.

4.4. NO_2 Concentration ($\mu g/m^3$)

The images show NO_2 concentration ($\mu g/m^3$) in the outdoor spaces of Golden Lane Estate (Figure 7). NO_2, or nitrogen dioxide, is a brown gas produced during fuel combustion processes, such as the use of petrol or diesel in vehicle engines, or natural gas in domestic heating [79]. NO_2 has both health and environmental impacts: breathing air with high concentrations of this gas can irritate airways and worsen respiratory conditions like asthma and allergies [80,81]. Additionally, when NO_2 interacts with water, oxygen, and other chemicals in the atmosphere, it can contribute to the formation of acid rain and air haze.

The results from fieldwork measurements and ENVI-met simulations indicate elevated levels of pollutant concentration along the streets surrounding Golden Lane Estate. Since motor vehicles are one of the major sources of NO_2 pollutants, the busiest street in the area, Goswell Road, exhibits the highest concentrations. Conversely, the spaces between the courtyards, which are primarily pedestrian areas, show low concentrations, except for the driveway area in Courtyard 2, where parked cars contribute to increased NO_2 levels. By comparing the ENVI-met simulation representing the real and no-vegetation scenarios, a strong correlation between NO_2 concentration and the presence of vegetation becomes apparent. This is particularly evident along Fann Street and Goswell Road, where the canopies of trees, by reducing wind flow velocity, trap pollutants and lead to increased NO_2 concentrations.

4.5. $PM_{2.5}$ and PM_{10} Concentration ($\mu g/m^3$)

The images display the concentration of $PM_{2.5}$ and PM_{10} ($\mu g/m^3$) in the outdoor spaces of Golden Lane Estate (Figures 8 and 9). PM, or particulate matter, refers to a mixture of solid and liquid materials with varying sizes, ranging from a few nanometres to around 100 micrometres. Primary particles are directly emitted from specific sources, while secondary particles are formed through chemical reactions in the atmosphere. The main sources of primary particles include emissions from road transport during the combustion of solid and liquid fuels; road dust; and the burning of fuels for industrial, commercial, and domestic purposes [79]. Long-term exposure to particulate matter can lead to respiratory and cardiovascular illnesses and can even cause death, particularly among individuals with pre-existing lung or heart conditions [82].

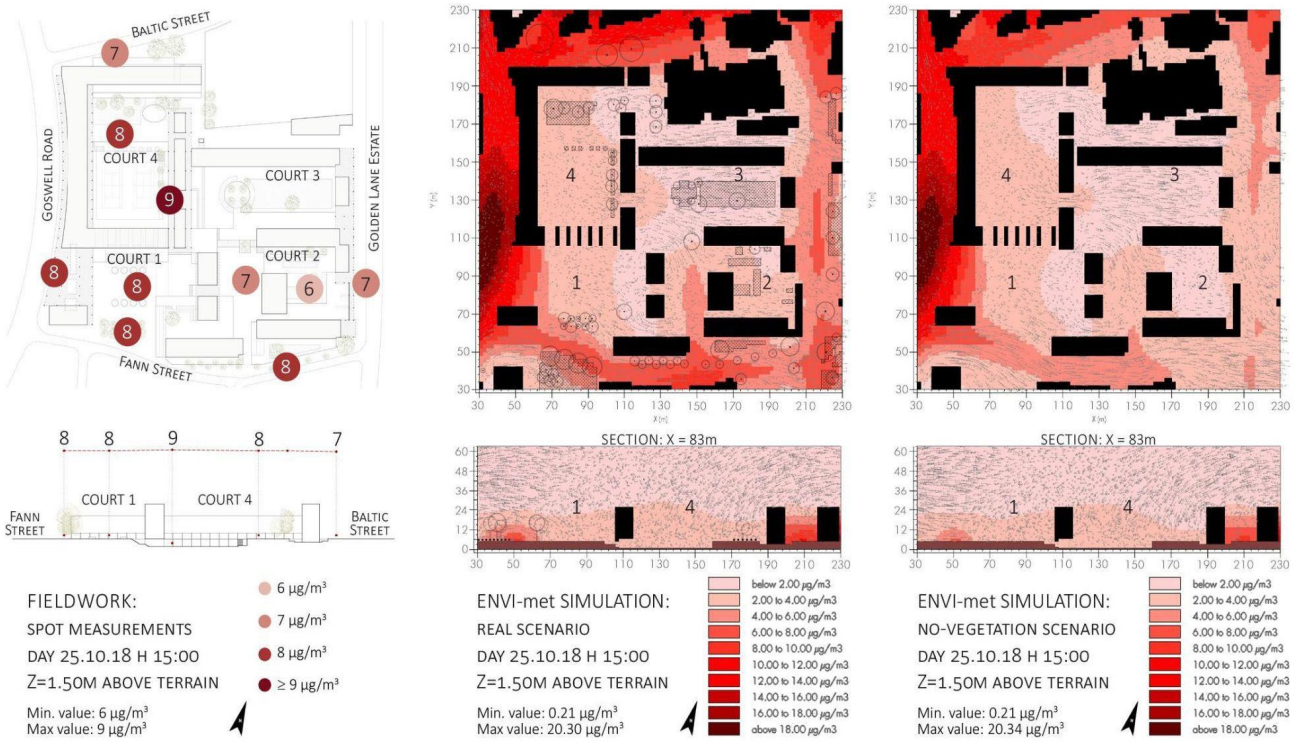

Figure 8. $PM_{2.5}$ concentration: (**left**) Fieldwork measurement, (**centre**) ENVI-met current scenario simulation, (**right**) ENVI-met no-vegetation scenario simulation.

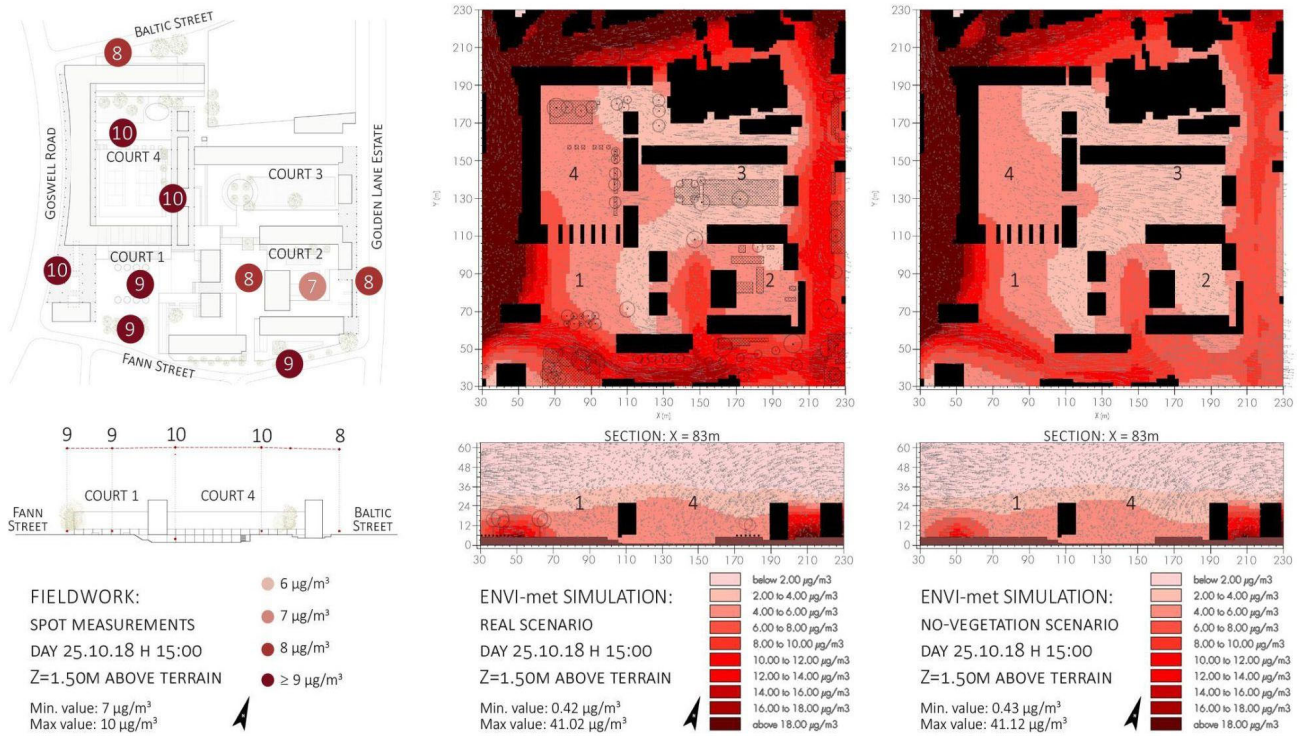

Figure 9. PM_{10} concentration: (**left**) Fieldwork measurement, (**centre**) ENVI-met current scenario simulation, (**right**) ENVI-met no-vegetation scenario simulation.

Analysing the images, it can be observed that the concentrations of particulate matter are higher along the perimeter of the Estate. Similar to NO_2, this phenomenon can be attributed to the presence of cars, which act as the main source of pollutants in this area.

The following section will discuss how the urban form and vegetation influence the local microclimate and impact air quality at a hyperlocal scale.

5. Discussion

One of the expected findings from the analysis is that the values measured during the fieldwork, such as air temperature (°C), relative humidity (%), wind velocity (m/s), and pollutant concentrations of PM_{10}, $PM_{2.5}$, and $NO_{2\ (\mu g/m^3)}$, differ from the data obtained from meteorological and air monitoring stations (Table 7).

Table 7. Data comparison on 25 October 2018 (h 15:00). Spot measurements in Golden Lane Estate (mean values) vs. data measured by meteorological station from London St. James' Park and pollutants station from London Sir John Cass School.

Type of Measurement	T (°C)	RH (%)	WS aver. (m/s)	$PM_{2.5}$ ($\mu g/m^3$)	PM_{10} ($\mu g/m^3$)	NO_2 ($\mu g/m^3$)
On-site spot measurements	15.0	59.9	1.0	8	10	16
Meteorological stations	13.3	70.0	4.0	11	22	59

These differences were anticipated, as the background concentration data for pollutants and meteorological data used in ENVI-met were extracted from meteorological and air monitoring stations located 3.8 and 1.7 km away from the study site, respectively. To enhance the accuracy and resolution of the computational fluid dynamics (CFD) model, the simulation was run for a total of 12 h. As the on-site spot measurements were conducted for only a few hours, with each measurement being instantaneous or lasting up to three minutes, the missing data for the entire 12 h ENVI-met simulation period were collected from the nearest air monitoring and meteorological stations to the site. Additionally, several simplifications and assumptions had to be made while modelling the site in ENVI-met. Another factor contributing to the variation in results could be the use of portable instruments for this study. Portable instruments may indicate slight differences (higher or lower) in their measurements compared to fixed monitoring stations. Furthermore, the impact of urban form on the microclimate of a specific urban location at a hyperlocal scale is distinctively unique and can vary from one location to another.

It is important to note that, except for air temperature, the on-site measurements consistently showed lower values compared to those calculated in ENVI-met. The spot measurements recorded values fluctuating between 14 °C and 16 °C, while the ENVI-met simulations generally indicated lower values ranging from 10.5 °C to 12.5 °C. One possible explanation for this difference could be the data extracted from St. James Park weather station, which was used as the source of meteorological data for the computational simulation. St. James Park is located in a highly vegetated area (Figure 10), and previous studies have demonstrated that areas close to parks and green infrastructure tend to be cooler compared to areas with low albedo materials and impervious surfaces [45,83,84]. The presence of a large volume of vegetation and trees can lower air and surface temperatures by providing shade and through evapotranspiration. In the case of St. James Park's weather station, the decrease in temperature is primarily due to evapotranspiration rather than the shade provided by trees. Another important factor to consider is the location of the weather monitoring site in an open space with no surrounding obstacles. This encourages a larger volume of air exchange and, consequently, higher wind velocity/flow, leading to further cooling of the surrounding area. This scenario is quite different from Golden Lane, where 87% of the area consists of impervious surfaces, and only 13% comprises greenery.

Figure 10. Meteorological station, London St. James Park.

However, one of the most relevant aspects of this comparative study is the broad correspondence between the pattern of measured and simulated data, particularly in relation to pollution concentration zones. This provides a possible starting point for further evaluating the impact of urban form and vegetation on air pollution dispersion. Another significant finding is the dependent correlation between the arrangement of buildings in Golden Lane Estate and the distribution of air pollution. The Estate is composed of residential blocks positioned perpendicularly to each other, and this layout appears to protect the inner courtyards from the infiltration of pollutant particles, which are predominantly concentrated along the streets surrounding the Estate. This phenomenon is particularly noticeable on Goswell Road and Baltic Street, where the continuous urban front of the buildings acts as an effective barrier in preventing pollutants from entering the Estate. A closer examination of the results reveals that the urban form, including solid and porous barriers and building arrangements, has an impact on temperature fluctuations, wind speeds, and wind directions, thereby influencing the air quality within street canyons of varying aspect ratios (H/W). According to Hussain, Lee, and Oke [85,86], the flow pattern in the street canopy layer is influenced by the wind direction at the roof height (urban canopy layer) and the aspect ratio (H/W) of the canyon. Consequently, perpendicular wind directions approaching the canyons can be described by three distinct flow regimes based on variations in the height and width of the street canyons: (i) isolated roughness flow, (ii) wake interference flow, and (iii) skimming flow (Table 8).

Table 8. Flow regimes type and characteristics in equal building heights canyons.

Flow Regime	Height-to-Width Ratio (H/W)	Characteristics
(i) Isolated roughness flow	H/W < 0.5	The flow fields surrounding the buildings on either side of the street do not interact. Two co-rotative vortices can be formed.
(ii) Wake interference flow	0.5 < H/W < 0.65	The flow around the upstream buildings starts to interfere with flow around downstream buildings. One main vortex can be formed.
(iii) Skimming flow	H/W > 0.65	The air above buildings hardly can interfere with the flow around downstream buildings inside the canyon. Circulatory or contra-rotative vortices can be formed.

The observed wind direction during the field measurements was from the southwest (SW) direction. Due to the surrounding blocks of buildings in Golden Lane, this has created a mixed microclimate with varying degrees of heat and pollution retention or flushing within the courtyards. This is closely related to the wind direction and its velocity. For instance, Courtyard 1, characterised by an uneven canyon of buildings with an overall aspect ratio of 0.58 (in the weak interference flow regime), has a leeward aspect ratio of 0.2 and a windward height-to-width ratio of 0.8. This configuration has resulted in a downdraft effect [87] on the windward facades of the tall building on the eastern side of the courtyard. Additionally, the southwest wind direction has induced positive pressure on

the two sides of the slab-like tall building (Figure 11), leading to parallel airflow around the building [88]. The ENVI-met simulation also supports these observations, demonstrating a significant improvement in air exchange and ventilation at the pedestrian level. Consequently, the levels of air pollution, specifically, NO_2 and PMs, have decreased compared to the other courtyards.

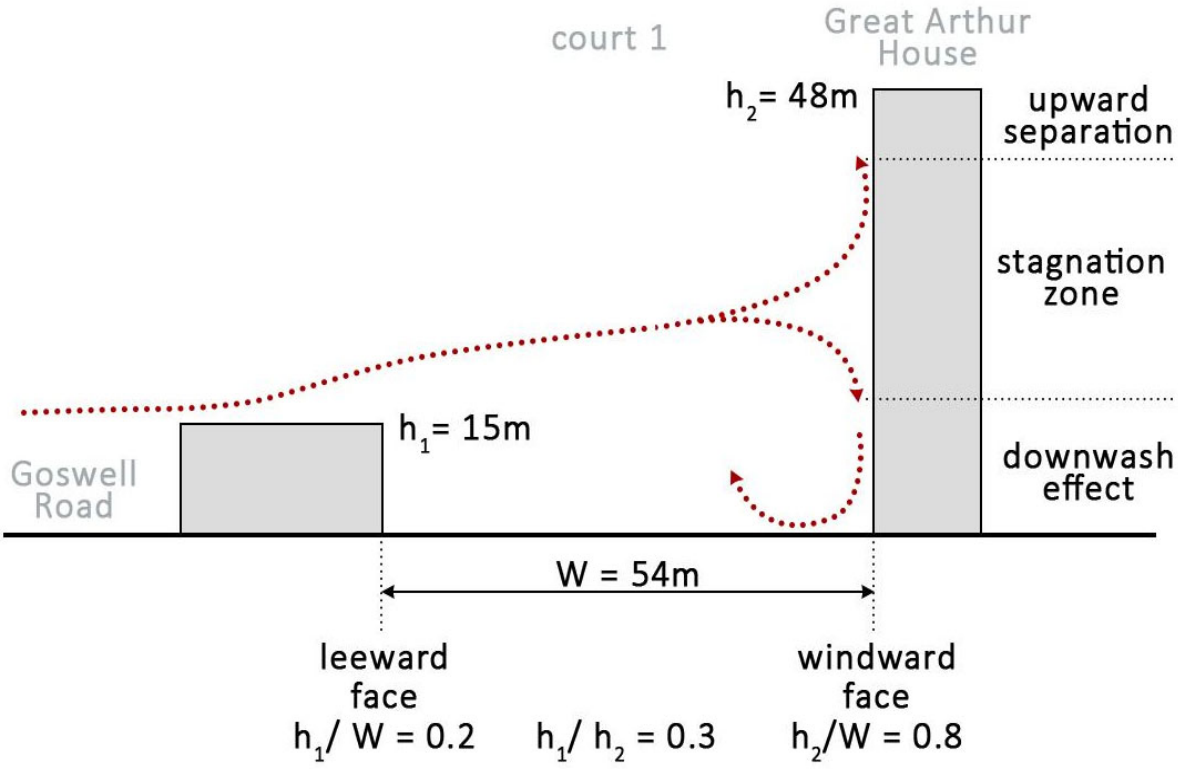

Figure 11. Courtyard 1 Golden Lane—2D flows with unequal building heights (asymmetric street canyon).

Perhaps the most intriguing finding can be observed in Courtyard 3. This courtyard consists of two buildings of equal height on its south and north sides, with an aspect ratio of 0.6, enclosed by two lower-height buildings of unequal heights on the west and east sides. The urban canyons on the west and east sides have a leeward aspect ratio of 0.07 and a windward aspect ratio of 0.18 (Figure 12). Consequently, winds coming from the favourable westerly direction can effectively flush out stagnant pollution from Courtyard 3. The ENVI-met simulation results also demonstrate a reduction in air pollution levels within the courtyard.

Furthermore, the location and height of the building on the west side of Courtyard 4 (tennis court) play a crucial role in providing cleaner air for Courtyard 3. This building, with its appropriate height and length, effectively blocks incoming pollution from Goswell Road. However, Courtyard 4 exhibits higher pollution levels compared to Courtyard 3. One possible explanation for this is that the pollution dispersed by the downdraft created by the Great Arthur House seems to be funnelled through the nearby narrow pedestrian passage, resulting in a pocket of polluted air in normally occupied areas (Courtyard 4, tennis court) (Figure 13). The aspect ratio of the leeward and windward sides of Courtyard 4 also contributes to the concentration of pollution at a hyperlocal scale (Figure 14).

As mentioned earlier, this study was conducted during the autumn period. While the results are promising, further research should be carried out during the summer period, when the scenarios mentioned above may be exacerbated due to an increase in vegetation Leaf Area Density (LAD). Additionally, more attention should be given to the shape and size of vegetation and their impact on pollution concentration and dispersion.

For instance, planting trees with a high Leaf Area Density (LAD) and heart-shaped or spherical crown shapes, with low clear stem height and minimal spacing between them, could potentially reduce air velocity at the pedestrian level and increase the concentration of pollutants [89]. Furthermore, as mentioned earlier, a discrepancy was observed between the values collected during on-site spot measurements and those obtained from ENVI-met simulations during the analysis of the results. To address this, future improvements to the methodology could involve the use of data logger instruments that can detect and record microclimatic variables and pollutant concentrations over a 24 h period, as required by ENVI-met. Despite the relatively limited data, this study provides valuable insights into the impact of porous (vegetation) and solid barriers on increasing or dispersing pollution levels in active urban areas. It is important to clarify that the removal of vegetation in the second simulated scenario should not be considered as a potential project proposal. Greenery, as mentioned in the introduction, offers a range of benefits, from economic to ecological and environmental. The simulation of the scenario without vegetation was solely conducted to better understand how the presence of vegetation affects pollutant concentrations in the built environment.

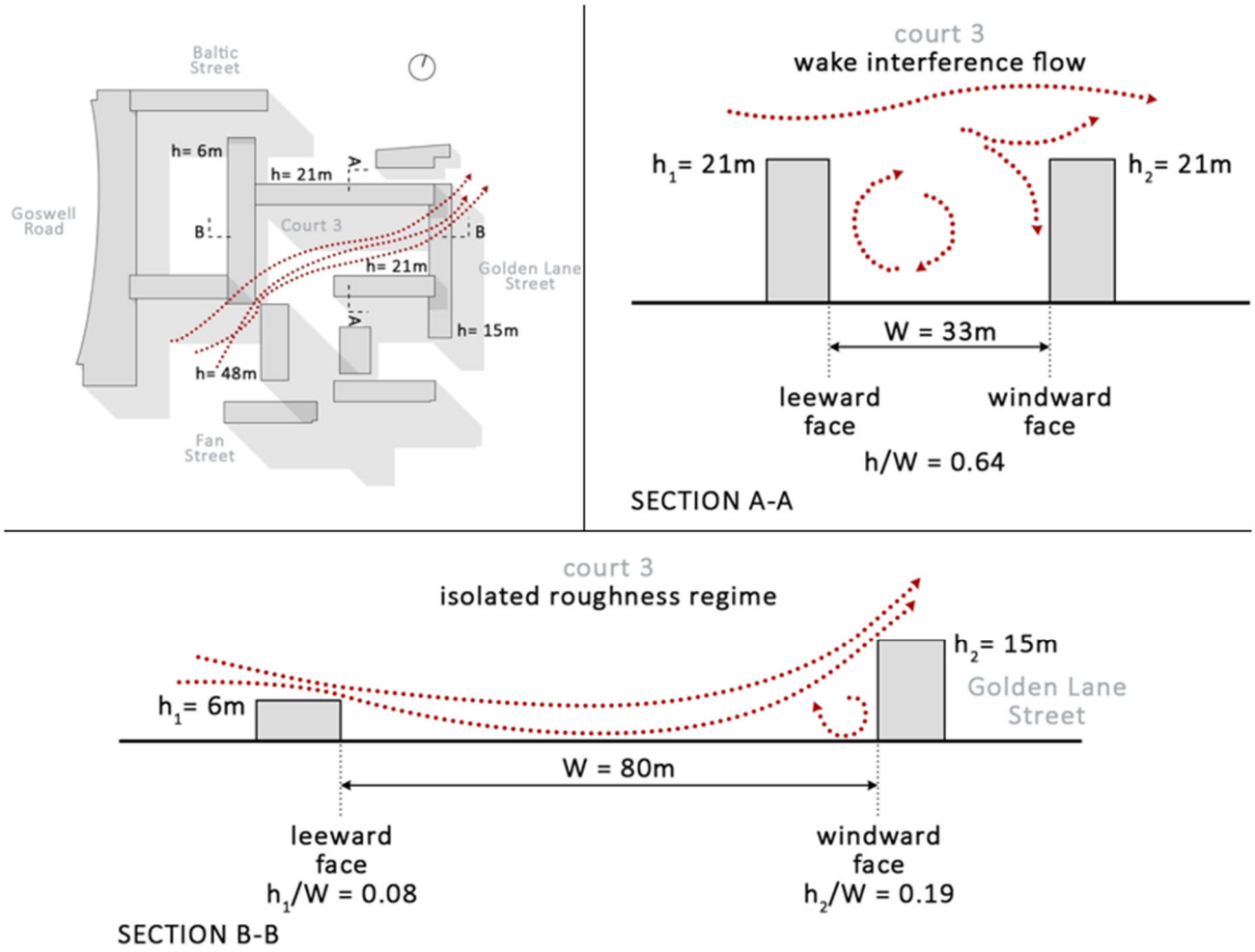

Figure 12. Courtyard 3 Golden Lane—2D flows with unequal building heights (asymmetric street canyon) on the west and east side and two buildings of equal height (symmetric street canyon) on its south and north sides.

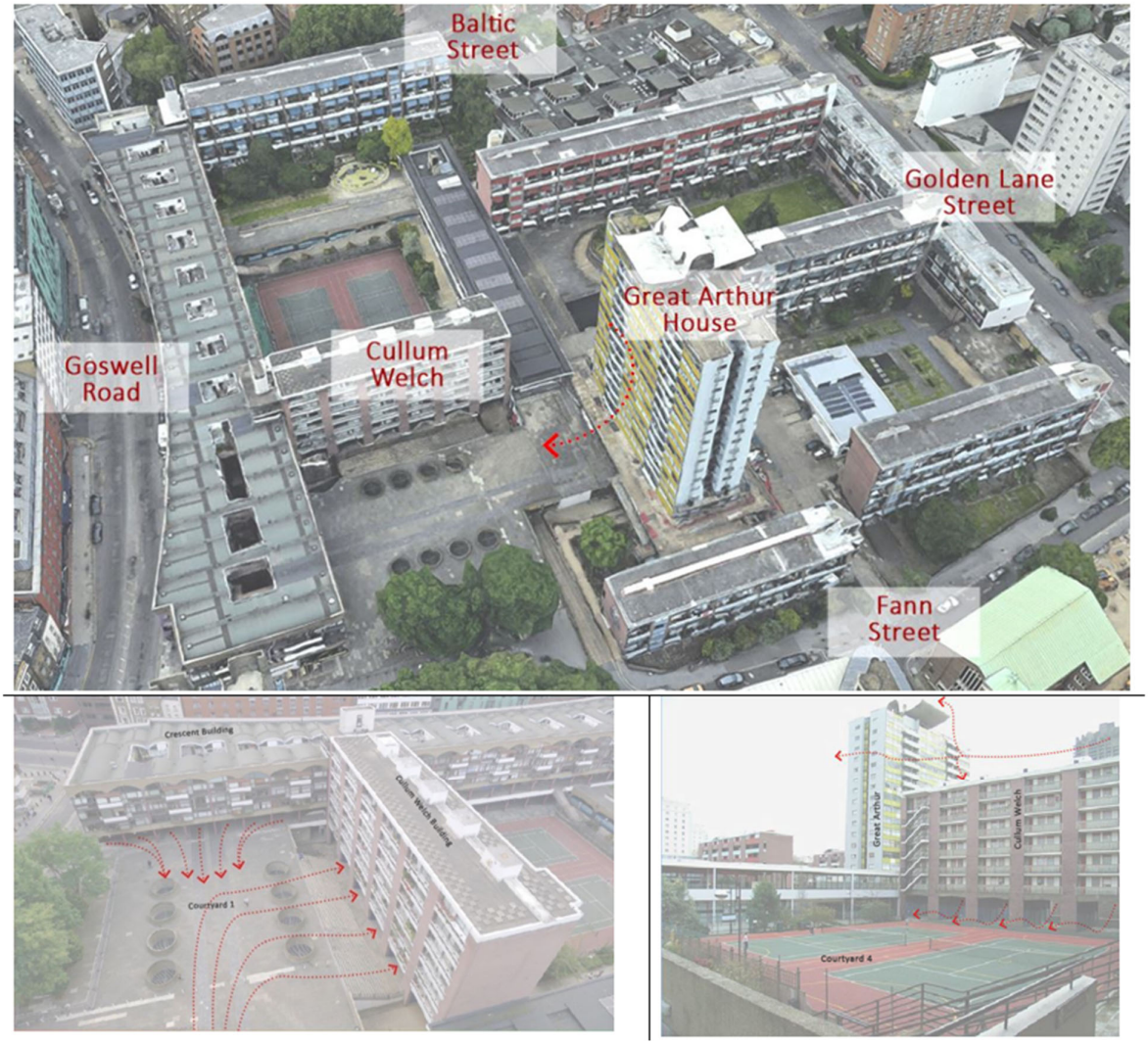

Figure 13. Courtyards 3 and 4 Golden Lane—Pollution, which has been dispersed by the downdraught created by the Great Arthur House, appears to be channelled through the nearby narrow pedestrian passage, creating a pocket of polluted air in usually occupied spaces (Courtyard 4, tennis court).

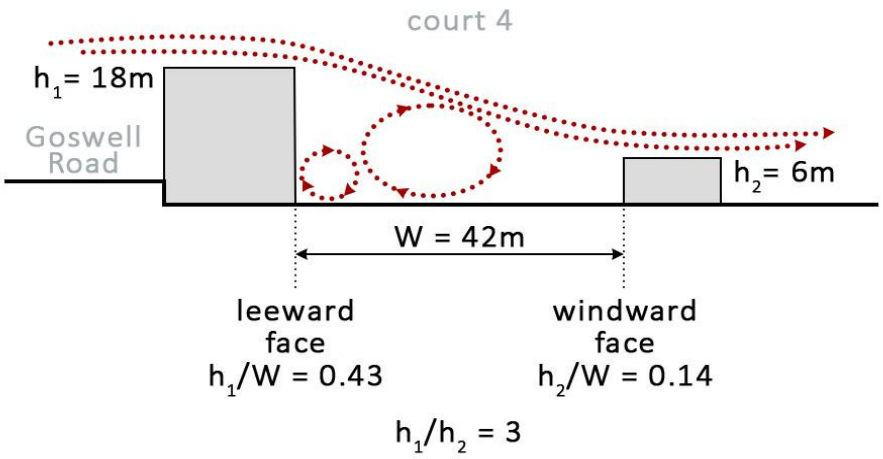

Figure 14. Courtyard 4 Golden Lane—2D flows with unequal building heights, which has induced the concentration of pollution.

6. Conclusions

Based on the results of the fieldwork and ENVI-met simulations conducted for both the current and no-vegetation scenarios, it is evident that the presence of vegetation and the aspect ratio of street canyons within courtyards can influence air pollution levels at a hyperlocal scale. A comparison between the current scenario and the no-vegetation scenario simulated using ENVI-met software v.4.4 revealed that vegetation and building arrangements have a significant impact on wind speed and direction, thereby affecting air pollution levels inside street canyons with different aspect ratios (H/W).

One notable finding from this study was the downdraught effect of tall buildings, which helped reduce and disperse pollution levels, leading to a considerable improvement in air exchange and ventilation at the pedestrian level. This resulted in a significant drop in air pollution levels. However, in the case of Golden Lane Estate, the dispersed pollution, influenced by the downdraught created by the tower, seemed to be funnelled through nearby narrow pedestrian passages, creating pockets of polluted air in typically occupied spaces, such as the tennis court, and increasing public exposure to polluted air.

These findings suggest that when measuring and modelling air pollution concentration, greater attention should be given to urban physical features at a hyperlocal scale, particularly in active urban areas with higher population density. Understanding the relationship between urban form and air pollution concentration in these areas is crucial. For the purpose of obtaining a general understanding of pollutant dispersion in a given area, scenario modelling and simulation of case study sites can be an effective method to aid decision making and extract more insights from design precedents.

ENVI-met is a leading simulation tool of urban microclimates, and it is commonly used by designers and planners to support decision making. It can be used to compare different options for green spaces and building layouts by performing detailed analysis of microclimatic conditions within urban areas, both in terms of building heating or cooling and human thermal comfort. Despite its extensive use over the past decade, some studies have underlined some limitations and needed simplifications [90–93] in the use of ENVI-met software v.4.4.

Furthermore, it is important to note that Outdoor Microclimate Maps (OMMs) offer a more accessible and understandable way to visualise output data of this nature. OMMs can serve as a tool for communicating a project's potential and enhancing the general understanding of the analysed phenomena among stakeholders, local administrations, and citizens.

In conclusion, this case study analysis serves as a foundation for future research on urban air pollution concentration at a hyperlocal scale across various urban settings and as a useful illustration for architects and designers of the complexity of interaction between built form and vegetation placement.

Author Contributions: All authors contributed to the study conception and planned the research. Material preparation, data collection, and analysis were performed by M.B., G.T. and M.M., M.M. and G.T. performed the ENVI-met simulation and modelling, and M.B. and R.S.-P. contributed to the interpretation of the results. M.B. took the lead in writing, wrote the major part of the manuscript, and revised the first draft of the manuscript, which was written by G.T. and M.M., R.S.-P. was involved in planning and supervising the work and worked on the manuscript. All authors discussed the results and contributed to the final manuscript. All authors have read and agreed to the published version of the manuscript.

Funding: This research received no external funding.

Institutional Review Board Statement: Not applicable.

Informed Consent Statement: Not applicable.

Data Availability Statement: All data generated or analysed during this study are included in this published article.

Acknowledgments: The authors would like to thank the University of Westminster for providing instruments and high-performance computing facilities to conduct this research. We thank the University of Bologna for their support throughout this research collaboration.

Conflicts of Interest: The authors declare that they have no conflicts of interest.

References

1. European Commission. Recovery Plan for Europe. 2021. Available online: https://commission.europa.eu/strategy-and-policy/recovery-plan-europe_en (accessed on 8 July 2023).
2. Amaral, A.R.; Rodrigues, E.; Rodrigues Gaspar, A.; Gomes, Á. Review on performance aspects of nearly zero-energy districts. *Sustain. Cities Soc.* **2018**, *43*, 406–420. [CrossRef]
3. Cheng, C.; Albert-Seifried, V.; Aelenei, L.; Vandevyvere, H.; Seco, S.; Sánchez, M.N.; Hukkalainen, M. A systematic approach towards mapping stakeholders in different phases of PED development—Extending the PED toolbox. In *Sustainability in Energy and Buildings 2021*; Littlewood, J.R., Howlett, R.J., Jain, L.C., Eds.; Smart Innovation, Systems and Technologies; Springer: Singapore, 2022; Volume 263, pp. 447–463. [CrossRef]
4. Olivadese, R.; Alpagut, B.; Revilla, B.P.; Brouwer, J.; Georgiadou, V.; Woestenburg, A.; van Wees, M. Towards Energy Citizenship for a Just and Inclusive Transition: Lessons Learned on Collaborative Approach of Positive Energy Districts from the EU Horizon2020 Smart Cities and Communities Projects. *Proceedings* **2021**, *65*, 20. [CrossRef]
5. World Health Organization (WHO). 9 Out of 10 People Worldwide Breathe Polluted Air, but More Countries Are Taking Action. 2018. Available online: https://www.who.int/news/item/02-05-2018-9-out-of-10-people-worldwide-breathe-polluted-air-but-more-countries-are-taking-action (accessed on 7 May 2022).
6. World Health Organization. WHO's First Global Conference on Air Pollution and Health. 2018. Available online: https://www.who.int/news-room/events/detail/2018/10/30/default-calendar/who-s-first-global-conference-on-air-pollution-and-health (accessed on 13 February 2020).
7. Hedman, Å.; Rehman, H.U.; Gabaldón, A.; Bisello, A.; Albert-Seifried, V.; Zhang, X.; Guarino, F.; Grynning, S.; Eicker, U.; Neumann, H.M.; et al. IEA EBC Annex83 positive energy districts. *Buildings* **2021**, *11*, 130. [CrossRef]
8. Sareen, S.; Albert-Seifried, V.; Aelenei, L.; Reda, F.; Etminan, G.; Andreucci, M.B.; Kuzmic, M.; Maas, N.; Seco, O.; Civiero, P.; et al. Ten questions concerning positive energy districts. *Build. Environ.* **2022**, *216*, 109017. [CrossRef]
9. Tuerk, A.; Frieden, D.; Neumann, C.; Latanis, K.; Tsitsanis, A.; Kousouris, S.; Llorente, J.; Heimonen, I.; Reda, F.; Ala-Juusela, M.; et al. Integrating plus energy buildings and districts with the eu energy community framework: Regulatory opportunities, barriers and technological solutions. *Buildings* **2021**, *11*, 468. [CrossRef]
10. COST Action 'PED-EU-NET'. PED Database. Available online: https://pedeu.net/map/ (accessed on 15 November 2023).
11. European Environment Agency (EEA). How Air Pollution Affects Our Health. 2023. Available online: https://www.eea.europa.eu/en/topics/in-depth/air-pollution/eow-it-affects-our-health#:~:text=Both%20short-%20and%20long-term,asthma%20and%20lower%20respiratory%20infections (accessed on 15 November 2023).
12. EEA Report. Unequal Exposure and Unequal Impacts: Social Vulnerability to Air Pollution, Noise and Extreme Temperatures in Europe. 2018. Available online: https://www.eea.europa.eu/publications/unequal-exposure-and-unequal-impacts (accessed on 15 November 2023).
13. Yang, J.; Shi, B.; Zheng, Y.; Shi, Y.; Xia, G. Urban form and air pollution disperse: Key indexes and mitigation strategies. *Sustain. Cities Soc.* **2020**, *57*, 101955. [CrossRef]
14. Viecco, M.; Jorquera, H.; Sharma, A.; Bustamante, W.; Fernando, H.J.S.; Vera, S. Green roofs and green walls layouts for improved urban air quality by mitigating particulate matter. *Build. Environ.* **2021**, *204*, 108120. [CrossRef]
15. Baradaran Motie, M.; Yeganeh, M.; Bemanian, M. Assessment of greenery in urban canyons to enhance thermal comfort & air quality in an integrated seasonal model. *Appl. Geogr.* **2023**, *151*, 102861. [CrossRef]
16. Baek, J.I.; Ban, Y.U. The Impacts of Urban Air Pollution Emission Density on Air Pollutant Concentration Based on a Panel Model. *Sustainability* **2020**, *12*, 8401. [CrossRef]
17. Buccolieri, R.; Santiago, J.-L.; Rivas, E.; Sáanchez, B. Reprint of: Review on urban tree modelling in CFD simulations: Aerodynamic, deposition and thermal effects. *Urban For. Urban Green.* **2018**, *37*, 56–64. [CrossRef]
18. Cardelino, C.A.; Chameides, W.L. Natural hydrocarbons, urbanization, and urban ozone. *J. Geophys. Res.* **1990**, *95*, 13971–13979. [CrossRef]
19. Berardi, U.; GhaffarianHoseini, A.; GhaffarianHoseini, A. State-of-the-art analysis of the environmental benefits of green roofs. *Appl. Energy* **2014**, *115*, 411–428. [CrossRef]
20. Taha, H. Modeling impacts of increased urban vegetation on ozone air quality in the South Coast Air Basin. *Atmos. Environ.* **1996**, *30*, 3423–3430. [CrossRef]
21. Abhijith, K.; Gokhale, S. Passive control potentials of trees and on-street parked cars in reduction of air pollution exposure in urban street canyons. *Environ. Pollut.* **2015**, *204*, 99–108. [CrossRef] [PubMed]
22. Amorim, J.; Rodrigues, V.; Tavares, R.; Valente, J.; Borrego, C. CFD modelling of the aerodynamic effect of trees on urban air pollution dispersion. *Sci. Total Environ.* **2013**, *461–462*, 541–551. [CrossRef] [PubMed]

23. CLAIRO Project. Green Infrastructure and Its Effect on Air Quality. Methodology of Planting Greenery in Urban Areas in Order to Capture Pollution. 2022. Available online: https://uia-initiative.eu/sites/default/files/2022-04/CLAIRO_Methodology_ENG.pdf (accessed on 15 November 2023).
24. Wang, Y.; Akbari, H. The effects of street tree planting on Urban Heat Island mitigation in Montreal. *Sustain. Cities Soc.* **2016**, *27*, 122–128. [CrossRef]
25. Loughner, C.P.; Allen, D.J.; Zhang, D.L.; Pickering, K.E.; Dickerson, R.R.; Landry, L. Roles of urban tree canopy and buildings in urban heat island effects: Parameterization and preliminary results. *J. Appl. Meteorol. Climatol.* **2012**, *51*, 1775–1793. [CrossRef]
26. Duarte, D.H.S.; Shinzato, P.; Gusson, C.d.S.; Alves, C.A. The impact of vegetation on urban microclimate to counterbalance built density in a subtropical changing climate. *Urban Clim.* **2015**, *14*, 224–239. [CrossRef]
27. Livesley, S.J.; McPherson, E.G.; Calfapietra, C. The Urban Forest and Ecosystem Services: Impacts on Urban Water, Heat, and Pollution Cycles at the Tree, Street, and City Scale. *J. Environ. Qual.* **2016**, *45*, 119–124. [CrossRef]
28. Bach, W. Urban Climate, Air Pollution and Planning. In *Urbanization and Environment: The Physical Geography of the City*; Detwyler, T.R., Marcus, M.G., Eds.; Duxbury Press: North Scituate, MA, USA; pp. 69–96.
29. Huang, J.Y.; Black, T.A.; Jassal, R.S.; Lavkulich, L.M.L. Modelling rainfall interception by urban trees. *Can. Water Resour. J.* **2017**, *42*, 336–348. [CrossRef]
30. Li, W.C.; Yeung, K.K.A. A comprehensive study of green roof performance from environmental perspective. *Int. J. Sustain. Built Environ.* **2014**, *3*, 127–134. [CrossRef]
31. Castiglia Feitosa, R.; Wilkinson, S.J. Attenuating heat stress through green roof and green wall retrofit. *Build. Environ.* **2018**, *140*, 11–22. [CrossRef]
32. Wong, N.H.; Cheong, D.K.W.; Yan, H.; Soh, J.; Ong, C.L.; Sia, A. The effects of rooftop garden on energy consumption of a commercial building in Singapore. *Energy Build.* **2003**, *35*, 353–364. [CrossRef]
33. Jaffal, I.; Ouldboukhitine, S.E.; Belarbi, R. A comprehensive study of the impact of green roofs on building energy performance. *Renew. Energy* **2012**, *43*, 157–164. [CrossRef]
34. Wong, N.H.; Kwang Tan, A.Y.; Chen, Y.; Sekar, K.; Tan, P.Y.; Chan, D.; Chiang, K.; Wong, N.C. Thermal evaluation of vertical greenery systems for building walls. *Build. Environ.* **2010**, *45*, 663–672. [CrossRef]
35. Azkorra, Z.; Pérez, G.; Coma, J.; Cabeza, L.F.; Bures, S.; Álvaro, J.E.; Erkoreka, A.; Urrestarazu, M. Evaluation of green walls as a passive acoustic insulation system for buildings. *Appl. Acoust.* **2015**, *89*, 46–56. [CrossRef]
36. Van Renterghem, T.; Hornikx, M.; Forssen, J.; Botteldooren, D. The potential of building envelope greening to achieve quietness. *Build. Environ.* **2013**, *61*, 34–44. [CrossRef]
37. Othman, N.; Mohamed, N.; Ariffin, M.H. Landscape Aesthetic Values and Visiting Performance in Natural Outdoor Environment. *Procedia Soc. Behav. Sci.* **2015**, *202*, 330–339. [CrossRef]
38. Zhou, X.; Rana, M.M.P. Social benefits of urban green space: A conceptual framework of valuation and accessibility measurements. *Manag. Environ. Qual.* **2012**, *23*, 173–189. [CrossRef]
39. Oke, T.R. Canyon geometry and the nocturnal heat island: Comparison of scale model and field observations. *J. Climatol.* **1981**, *29*, 237–254. [CrossRef]
40. Givoni, B. *Climate Considerations in Buildings and Urban Design*; Van Nostrand Reinhold: New York, NY, USA, 1998.
41. Santamouris, M. Environmental Planning in Urban Areas. Generalisation based on least squared adjustments. *Proc. Int. Arch. Photogramm. Remote Sens.* **2000**, 931–938.
42. Cole, R.J. Designing High-Density Cities. In *Designing High-Density Cities for Social and Environmental Sustainability*; Ng, E., Ed.; Routledge: London, UK, 2009.
43. Edussuriya, P.; Chan, A.; Ye, A. Urban morphology and air quality in dense residential environments in Hong Kong. Part I: District-level analysis. *Atmos. Environ.* **2011**, *45*, 4789–4803. [CrossRef]
44. Ren, C.; Ng, E.Y.Y.; Katzschner, L. Urban climatic map studies: A review. *Int. J. Climatol.* **2011**, *31*, 2213–2233. [CrossRef]
45. Ng, E.; Chen, L.; Wang, Y.; Yuan, C. A study on the cooling effects of greening in a high-density city: An experience from Hong Kong. *Build. Environ.* **2012**, *47*, 256–271. [CrossRef]
46. Chatzidimitriou, A.; Yannas, S. Street canyon design and improvement potential for urban open spaces; the influence of canyon aspect ratio and orientation on microclimate and outdoor comfort. *Sustain. Cities Soc.* **2017**, *33*, 85–101. [CrossRef]
47. Jeanjean, A.; Buccolieri, R.; Eddy, J.; Monks, P.; Leigh, R. Air quality affected by trees in real street canyons: The case of Marylebone neighbourhood in central London. *Urban For. Urban Green.* **2017**, *22*, 41–53. [CrossRef]
48. Kazmierczak, A.; James, P. The Role of Urban Green Spaces in Improving Social Inclusion. In Proceedings of the 7th International Postgraduate Research Conference in the Built and Human Environment, Greater Manchester, UK, 28–29 March 2007.
49. Buccolieri, R.; Gao, Z.; Gatto, E.; Rui, L.; Ding, W. Study of the effect of green quantity and structure on thermal comfort and air quality in an urban-like residential district by ENVI-met modelling. *Build. Simul.* **2018**, *12*, 183–194. [CrossRef]
50. Mandal, M.; Popek, R.; Przybysz, A.; Roy, A.; Das, S.; Sarkar, A. Breathing Fresh Air in the City: Implementing Avenue Trees as a Sustainable Solution to Reduce Particulate Pollution in Urban Agglomerations. *Plants* **2023**, *12*, 1545. [CrossRef]
51. Hinds, W.C. Aerosol Technology: Properties, Behavior, and Measurement of Airborne Particles (Second ed.). 1999. Available online: http://library.navoiy-uni.uz/files/hinds%20w.c.%20-%20aerosol%20technology-%20properties,%20behavior,%20and%20measurement%20of%20airborne%20particles%20(2nd%20edition)(1999)(504s).pdf (accessed on 15 July 2023).

52. Petroff, A.; Mailliat, A.; Amielh, M.; Anselmet, F. Aerosol dry deposition on vegetative canopies. Part I: Review of present knowledge. *Atmos. Environ.* **2008**, *42*, 3625–3653. [CrossRef]
53. Nowak, D.J.; Crane, D.E. The Urban Forest Effects (UFORE) Model: Quantifying Urban Forest Structure and Functions. *For. Service.* **2000**, *8*, 714–720.
54. Barwise, Y.; Kumar, P. Designing vegetation barriers for urban air pollution abatement: A practical review for appropriate plant species selection. *NPJ Clim. Atmos. Sci.* **2020**, *3*, 12. [CrossRef]
55. Nowak, D.J.; Crane, D.E.; Stevens, J.C.; Ibarra, M. Brooklyn's Urban Forest. United States Department of Agriculture. 2002; 107. Available online: https://www.fs.usda.gov/ne/newtown_square/publications/technical_reports/pdfs/2002/gtrne290.pdf (accessed on 15 July 2023).
56. Tallis, M.; Taylor, G.; Sinnett, D.; Freer-Smith, P. Estimating the removal of atmospheric particulate pollution by the urban tree canopy of London, under current and future environments. *Landsc. Urban Plan.* **2011**, *103*, 129–138. [CrossRef]
57. Vos, P.E.J.; Maiheu, B.; Vankerkom, J.; Janssen, S. Improving local air quality in cities: To tree or not to tree? *Environ. Pollut.* **2013**, *183*, 113–122. [CrossRef] [PubMed]
58. Buccolieri, R.; Gromke, C.; Di Sabatino, S.; Ruck, B. Aerodynamic effects of trees on pollutant concentration in street canyons. *Sci. Total Environ.* **2009**, *407*, 5247–5256. [CrossRef] [PubMed]
59. Ehrnsperger, L.; Klemm, O. Air pollution in an urban street canyon: Novel insights from highly resolved traffic information and meteorology. *Atmos. Environ. X* **2022**, *13*, 100151. [CrossRef]
60. Santiago, J.L.; Rivas, E.; Sanchez, B.; Buccolieri, R.; Martin, F. The impact of planting trees on NOx concentrations: The case of the Plaza de la Cruz neighborhood in Pamplona (Spain). *Atmosphere* **2017**, *8*, 131. [CrossRef]
61. Carpentieri, M.; Robins, A.G. Influence of urban morphology on air flow over building arrays. *J. Wind Eng. Ind. Aerodyn.* **2015**, *145*, 61–74. [CrossRef]
62. Xie, X.; Huang, Z.; Wang, J.S. Impact of building configuration on air quality in street canyon. *Atmos. Environ.* **2005**, *39*, 4519–4530. [CrossRef]
63. Aristodemou, E.; Boganegra, L.M.; Mottet, L.; Pavlidis, D.; Constantinou, A.; Pain, C.; Robins, A.; ApSimon, H. How tall buildings affect turbulent air flows and dispersion of pollution within a neighbourhood. *Environ. Pollut.* **2018**, *233*, 782–796. [CrossRef]
64. City of London. Golden Lane Estate Listed Building Management Guidelines. 2013. Available online: https://www.cityoflondon.gov.uk/assets/Services-Environment/golden-lane-listed-building-management-guidelines.pdf (accessed on 8 July 2023).
65. Edussuriya, P.; Chan, A.; Malvin, A. Urban morphology and air quality in dense residential environments: Correlations between morphological parameters and air pollution at street-level. *J. Eng. Sci. Technol.* **2014**, *9*, 64–80.
66. Schiano-Phan, R.; Lau, B.; Pourel, D.; Khan-Phatan, S. Spatial Delight and Environmental Performance of Modernist Architecture in London—Golden Lane Estate. *Future Cities Environ.* **2018**, *4*, 782–796. [CrossRef]
67. Stewart, I.D.; Oke, T.R. 'Local climate zones' for urban temperature studies. *Bull. Am. Meteorol. Soc.* **2012**, *93*, 1879–1900. [CrossRef]
68. Department for UK Transport. Road Traffic Statistics. Road Traffic. 2018. Available online: https://roadtraffic.dft.gov.uk/#6/55.254/-6.064/basemap-regions-countpoints (accessed on 8 July 2023).
69. Buccolieri, R.; Salim, S.M.; Leo, L.S.; Di Sabatino, S.; Chan, A.; Ielpo, P.; de Gennaro, G.; Gromke, C. Analysis of local scale tree-atmosphere interaction on pollutant concentration in idealized street canyons and application to a real urban junction. *Atmos. Environ.* **2011**, *45*, 1702–1713. [CrossRef]
70. Gromke, C.; Ruck, B. Influence of trees on the dispersion of pollutants in an urban street canyon-Experimental investigation of the flow and concentration field. *Atmos. Environ.* **2007**, *41*, 3287–3302. [CrossRef]
71. Wania, A.; Bruse, M.; Blond, N.; Weber, C. Analysing the influence of different street vegetation on traffic-induced particle dispersion using microscale simulations. *J. Environ. Manag.* **2012**, *94*, 91–101. [CrossRef] [PubMed]
72. Ng, W.Y.; Chau, C.K. Evaluating the role of vegetation on the ventilation performance in isolated deep street canyons. *Int. J. Environ. Pollut.* **2012**, *50*, 98–110.
73. Gromke, C.; Ruck, B. Pollutant Concentrations in Street Canyons of Different Aspect Ratio with Avenues of Trees for Various Wind Directions. *Bound.-Layer Meteorol.* **2012**, *144*, 41–64. [CrossRef]
74. Johnson, O.; More, D. *Collins Tree Guide*; Harper Collins Publishers: New York, NY, USA, 2004.
75. Ozkeresteci, I.; Crewe, K.; Brazel, A.J.; Bruse, M. Use and evaluation of the ENVI-met model for environmental design and planning. An Experiment on Lienar Parks. In Proceedings of the 21st International Cartographic Conference (ICC), Durban, South Africa, 10–16 August 2003.
76. Salata, F.; Golasi, I.; Vollaro, A.D.L.; Vollaro, R.D.L. How high albedo and traditional buildings' materials and vegetation affect the quality of urban microclimate. A case study. *Energy Build.* **2015**, *99*, 32–49. [CrossRef]
77. Conry, P.; Sharma, A.; Potosnak, M.J.; Leo, L.S.; Bensman, E.; Hellmann, J.J.; Fernando, H.J.S. Chicago's heat island and climate change: Bridging the scales via dynamical downscaling. *J. Appl. Meteorol. Climatol.* **2015**, *54*, 1430–1448. [CrossRef]
78. Erell, E.; Pearlmutter, D.; Williamson, T. *Urban Microclimate*; Routledge: London, UK, 2010. [CrossRef]
79. WHO Report. Global Air Quality Guidelines. 2021. Available online: https://iris.who.int/bitstream/handle/10665/345329/9789240034228-eng.pdf?sequence=1 (accessed on 16 November 2023).

80. Zheng, X.; Orellano, P.; Lin, H.; Jiang, M.; Guan, W. Short-term exposure to ozone, nitrogen dioxide, and sulphur dioxide and emergency department visits and hospital admissions due to asthma: A systematic review and meta-analysis. *Environ. Int.* **2021**, *150*, 106435. [CrossRef]
81. Huangfu, P.; Atkinson, R. Long-term exposure to NO_2 and O_3 and all-cause and respiratory mortality: A systematic review and meta-analysis. *Environ. Int.* **2020**, *144*, 105998. [CrossRef] [PubMed]
82. Chen, J.; Hoek, G. Long-term exposure to PM and all-cause and cause-specific mortality: A systematic review and meta-analysis. *Environ. Int.* **2020**, *143*, 105974. [CrossRef] [PubMed]
83. Tsoka, S.; Tsikaloudaki, K.; Theodosiou, T. Urban space's morphology and microclimatic analysis: A study for a typical urban district in the Mediterranean city of Thessaloniki, Greece. *Energy Build.* **2017**, *156*, 96–108. [CrossRef]
84. Dimoudi, A.; Nikolopoulou, M. Vegetation in the Urban Environment. *Energy Build.* **2003**, *35*, 69–76. [CrossRef]
85. Hussain, M.; Lee, B.E. *An Investigation of Wind Forces on Three-Dimensional Roughness Elements in a Simulated Atmospheric Boundary Layer Flow. Part II: Flow Over Large Arrays of Identical Roughness Elements and the Effect of Frontal and Side Aspect Ratio Variations*; Department of Building Science, University of Sheffield: Sheffield, UK, 1980.
86. Oke, T.R. *Boundary Layer Climates*; Routledge: London, UK, 1987.
87. Ng, E.; Wong, H.H.; Han, M. Permeability, porosity and better ventilated design for high density cities. In Proceedings of the PLEA2006—The 23rd Conference on Passive and Low Energy Architecture, Geneva, Switzerland, 6–8 September 2006.
88. Lawson, T. *Building Aerodynamics*; Imperial College Press: London, UK; River Edge, NJ, USA, 2001.
89. Borna, M.; Schiano-Phan, R. Improving Hyperlocal Air Quality in Cities Impact of vegetation on pollutants concentration at pedestrian level. In Planning Post Carbon Cities. In Proceedings of the 35th PLEA Conference on Passive and Low Energy Architecture, A Coruña, Spain, 1–3 September 2020. Available online: https://westminsterresearch.westminster.ac.uk/download/f5536c70e251a5aa07cc722f2570ea32ccaaf84eca311088eac7b3087c8c0933/10707927/PLEA_2020_PlanningPostCarbonCities_Proc_Vol_1MB.pdf (accessed on 15 July 2023).
90. Cranck, P.J.; Sailor, D.J.; Ban-Weiss, J.; Taleghani, J. Evaluating the ENVI-met microscale model for suitability in analysis of targeted urban heat mitigation strategies. *Urban Clim.* **2018**, *26*, 188–197. [CrossRef]
91. Acero, J.A.; Arrizabalaga, J. Evaluating the performance of ENVI-met model in diurnal cycles for different meteorological conditions. *Theor. Appl. Climatol.* **2019**, *131*, 455–469. [CrossRef]
92. Oliveira Favretto, A.P.; Lucas Souza, L.C. A meta-analysis over geometric modeling simplifications in ENVI-met urban climate simulation. *Ambiente Construído* **2019**, *1*, 143–160. [CrossRef]
93. Alves, F.M.; Gonçalves, A.; del Caz-Enjuto, M.R. The Use of Envi-Met for the Assessment of Nature-Based Solutions' Potential Benefits in Industrial Parks—A Case Study of Argales Industrial Park (Valladolid, Spain). *Infrastructures* **2022**, *7*, 85. [CrossRef]